Successful Clinical Sequencing by Molecular Tumor Board in an Elderly Patient With Refractory Sézary Syndrome

Yasuki Hijikata, MD, PhD[1]; Kazuaki Yokoyama, MD, PhD[2]; Nozomi Yokoyama, MT[3]; Yasuo Matsubara, MD, PhD[1]; Eigo Shimizu[4]; Makoto Nakashima, PhD[5]; Makoto Yamagishi, PhD[5]; Yasunori Ota, MD, PhD[7]; Lay Ahyoung Lim, MD, PhD[1]; Rui Yamaguchi, PhD[4]; Mika Ito[6]; Yukihisa Tanaka, MT[7]; Tamami Denda, MS[7]; Kenzaburo Tani, MD[1]; Hiroshi Yotsuyanagi, MD[1]; Seiya Imoto, PhD[8]; Satoru Miyano, PhD[4]; Kaoru Uchimaru, MD, PhD[5]; and Arinobu Tojo, MD, PhD[2,8]

INTRODUCTION

Sézary syndrome (SS), a rare, aggressive, leukemic variant of cutaneous T-cell lymphoma (CTCL), comprises the malignant clonal proliferation of T lymphocytes, and is prone to skin involvement.[1] Most patients with SS are elderly, with erythroderma present on > 80% of the body. SS is rarely curable and has a poor prognosis; the median survival of patients with stage IV SS is approximately 2 years.[2] Recent SS genomic profiling with next-generation sequencing (NGS) demonstrated impaired normal signaling, which suggests the possibility of new treatment targets.[3]

NGS-based genomic testing for cancer is becoming more widespread as a clinical tool for accurate diagnosis and proper treatment in clinical oncology.[4] However, the use of various NGS techniques to guide cancer therapy has created challenges in analyzing large volumes of genomic data and reporting results to patients and caregivers.[5] To resolve this, we organized a clinical sequencing team called the molecular tumor board (MTB) at the Institute of Medical Science, The University of Tokyo. Clinical sequencing is associated with several potential challenges in analysis, interpretation, and drug development for rare cancers such as SS. Here, we report the use of clinical sequencing to achieve a complete response in an elderly patient with SS refractory to standard treatment.

CASE REPORT

A 75-year-old male was diagnosed with SS (T4N3M0B1b; stage IVA2) in 2015. He had received various treatments in multiple hospitals, including prednisone, psoralen and ultraviolet A, extracorporeal photopheresis, bexarotene, romidepsin, total skin electron beam therapy, brentuximab vedotin, interferon alfa-2b, methotrexate, and pembrolizumab, but skin lesions did not respond adequately. Severe pneumonia also occurred during methotrexate therapy and was resolved by intensive care. The patient was admitted to our hospital in November 2016. Generalized erythroderma, clinical stage IIIA, was observed. He received mogalizumab, low-dose VP-16, and local radiation therapy. Each resulted in temporal clinical responses, but with limited effects.

Our study protocol (No. 26-112-270402/28-17-0708; Appendix) was approved by our institutional review board and was in accordance with the Declaration of Helsinki. After obtaining written informed consent, whole-exome sequencing (WES) and RNA sequencing were performed on skin tumor biopsy samples on February 1, 2017, for comparisons with normal tissue, followed by analysis by our hospital curators (Appendix Figs A1 and A2). Specifically, from WES, 77 coding variants were identified (Appendix Table A1). Among these, the MTB inferred only one driver mutation in *TP53* (c.560-1G>A, splicing mutation, Appendix Table A1) from which no actionable molecular targets were identified. However, from RNA sequencing, actionable molecular targets were identified. We regarded the following gene upregulations as directly targetable: *CCR4* (mogalizumab), *LCK* (dasatinib), *CD274* as PD-L1 (PD-L1 inhibitors, pembrolizumab), *CTLA4* (ipilimumab), *IL2RA* as CD25 (denileukin diftitox), *TNFRSF8* as CD30 (brentuximab vedotin), and nuclear factor-κB (NF-κB) signaling pathway (Table 1). Of note, we also inferred lenalidomide as a potential therapeutic option on the basis of the following two reasons: The tumor was enriched in pathways that were all indirectly targetable by lenalidomide (eg, Kyoto Encyclopedia of Genes and Genomes [KEGG]-NF-κB signaling [Appendix Fig A7], KEGG-cytokine-cytokine receptor interaction [Appendix Fig A9], and KEGG-natural killer [NK]-cell–mediated cytotoxicity[6] [Appendix Fig A8], and KEGG-tumor necrosis factor [TNF] signaling [Appendix Fig A10] on the basis of the KEGG DRUG Database,[7] Therapeutic Target Database[8]), and documented efficacy of lenalidomide was reported in patients with CTCL with overall response rates of 28% in a phase II trial of monotherapy for refractory SS[9] and a phase III trial of maintenance therapy.[10]

Mogalizumab, pembrolizumab, and brentuximab vedotin had already been used during the patient's protracted clinical course. Denileukin diftitox was excluded because the latest immunohistochemical

ASSOCIATED CONTENT

Appendix

Author affiliations and support information (if applicable) appear at the end of this article.

Accepted on December 14, 2019 and published at ascopubs.org/journal/po on May 15, 2020: DOI https://doi.org/10.1200/PO.19.00254

TABLE 1. Actionable Alterations With Drug

Upregulated Gene	Drug	Reason of the Exclusion
CCR4	Mogalizumab	Drug resistance
LCK	Dasatinib	Lack of clinical evidence
PDL1	PD-L1 inhibitor	Drug resistance
CTLA4	Ipilimumab	Lack of consent
CD25	Denileukin diftitox	Lack of expression by immunohistochemistry
CD30	Brentuximab vedotin	Drug resistance
Activated signaling pathway		
NF-κB	Lenalidomide	MTB recommendation

NOTE. See also Table 2. Candidate genes and drugs selected by the MTB proposed the activated NF-κB pathway on the basis of gene set enrichment analysis results. The attending physician chose lenalidomide (off-label use) from this report.

Abbreviations: MTB, molecular tumor board; NF-κB, nuclear factor-κB.

analysis of the patient's lesions showed that they were CD25⁻. The two remaining candidates were ipilimumab and lenalidomide. The patient was reluctant to receive ipilimumab because its mechanism of action is similar to that of pembrolizumab. Therefore, we focused on lenalidomide as a therapeutic option.

To identify any potential predictive signatures of response to lenalidomide therapy in this patient, we investigated whether there could be any overlapping lenalidomide-related gene signatures in our in-house, independent RNA sequencing data set (Appendix Figs A2-A5). Specifically, we focused on available data from patients with adult T-cell leukemia/lymphoma (ATL), another mature/peripheral T-cell neoplasm in which lenalidomide demonstrated clinical efficacy with an overall response rate of 42% in a phase II study (ATLL-002 [ClinicialTrials.gov identifier: NCT01724177]). Gene expression data from tumors of two patients with ATL before lenalidomide therapy were available for this purpose; one patient (unique patient number [UPN] 1) had an objective response to lenalidomide therapy, whereas the other patient (UPN2) was primarily refractory to lenalidomide (the patient characteristics are listed in Appendix Table A2). To identify molecular signatures associated with lenalidomide response and to reduce bias derived from different diseases, such as ATL, we extracted differentially expressed genes from the tumor of UPN1 (responsive ATL case) compared with expression levels in the tumor from UPN2 (refractory ATL case). Overall, we found 1,250 and 1,197 genes upregulated in CTCL and the current ATL case, respectively.

KEGG pathway enrichment on the basis of the DAVID annotation tool revealed that 73 and 88 pathways were enriched in CTCL and ATL, respectively (Appendix Fig A3; Appendix Table A3). Among common pathways (n = 52), we identified HTLV-1 and lenalidomide target signatures (Appendix Fig A3, A7-A10; Appendix Table A3). Gene set enrichment analysis (GSEA) of panels of curated gene sets related to lenalidomide confirmed the enrichment of a signature predictive of response to lenalidomide in both CTCL and ATL. In contrast, neither signature of resistance was enriched in CTCL and ATL (Table 2). On the basis of these predictive signatures and documented efficacy in patients with CTCL,[9,10] we chose lenalidomide.

Beginning on September 11, 2017, lenalidomide was orally administered at a daily dose of 25 mg for 21 days of a 28-day cycle while the patient had clinical stage IIB disease (Fig 1A). After the first course of treatment, all skin tumors disappeared except for one on his sternal region (Fig 1B). In addition, a transient flare reaction (TFR) that presented as erythema around skin tumors was observed during the first course (Fig 1C). Aspiration pneumonia developed at the end of the first course, and thus, the dosage of the second course was reduced to 10 mg daily; it was subsequently increased by 5 mg every cycle to a maximum of 20 mg daily. We extended the interval course from 1 to 2 weeks according to the patient's status. Although new lesions disappeared after three courses of treatment, a 9-cm sternal tumor remained, but it was smaller than its previous size. It was later irradiated with 20 Gy in December 2017. The fifth course of lenalidomide was completed on February 3, 2017, and all tumors, including sternal lesions, disappeared completely (Fig 1D).

Upon immunohistochemical analysis of tumor specimens before and after lenalidomide treatment, a remarkable number of CD8⁺ cells and few CD25⁺ and Foxp3⁺ cells were observed in each skin tumor (Appendix Table A4; Appendix Fig A6). Especially, the number of CD8⁺ cells after the first course increased compared with that before the treatment but decreased in the treatment-resistant lesion after the third course of lenalidomide.

DISCUSSION

To our knowledge, this report is the first of successful clinical results in a patient with refractory SS treated with lenalidomide, which was selected on the basis of clinical sequencing. Advances in clinical sequencing have enabled the discovery of actionable alterations that yield clinical benefit.[11] Patients with advanced-stage SS have an unfavorable prognosis and an unmet clinical need for effective

TABLE 2. Lenalidomide-Related Gene Sets and Annotations

	Lenalidomide-Related Gene Sets and Annotations			Current Patient			A Lenalidomide-Responsive Patient With ATL		
Gene Set	Gene Size	Signature	Reference	NES	*P*	FDR *q*	NES	*P*	FDR *q*
HINATA_NFKB_IMMU_INF	17	Lenalidomide-responsive/ target pathway	TTD[8], KEGG DRUG/ pathway[7]	1.88	.004	0.008	1.55	.027	0.013
TIAN_TNF_SIGNALING_VIA_NFKB	25	Lenalidomide-responsive/ target pathway	TTD[8], KEGG DRUG/ pathway[7]	1.67	.005	0.025	1.36	.029	0.046
KEGG_NF-kappa_B_signaling_pathway	102	Lenalidomide-responsive/ target pathway	TTD[8], KEGG DRUG/ pathway[7]	1.93	.000	0.005	1.38	.017	0.033
KEGG_CYTOKINE_CYTOKINE_RECEPTOR_ INTERACTION	249	Lenalidomide-responsive/ target pathway	TTD[8], KEGG DRUG/ pathway[7]	1.75	.000	0.005	1.58	.000	0.009
KEGG_NATURAL_KILLER_CELL_MEDIATED_ CYTOTOXICITY	130	Lenalidomide-responsive/ target pathway	TTD[8], KEGG DRUG/ pathway[7]	1.73	.000	0.005	1.45	.003	0.018
KEGG_APOPTOSIS	86	Lenalidomide-responsive/ target pathway	TTD, KEGG DRUG/ pathway	1.44	.004	0.023	1.18	.118	0.114
Aue_CLL_lenalidomide_target_Th1immunity_ TableS1	155	Lenalidomide-responsive/ target pathway	Aue[17]	1.93	.000	0.009	1.94	.000	0
Bhutani_myeloma_lenalidomide_target_ genes_TableS2	147	Lenalidomide-responsive/ target pathway	Bhutani[18]	1.22	.035	0.104	1.60	.000	0.009
E2F3_UP.V1_UP	186	Lenalidomide resistance	Neri[19]	1.23	.029	0.284		NE	
KRAS.600.LUNG.BREAST_UP.V1_UP	271	Lenalidomide resistance	Neri[19]	1.23	.320	0.220	1.42		0.062
KRAS.KIDNEY_UP.V1_UP	139	Lenalidomide resistance	Neri[19]		NE			NE	
KRAS.LUNG_UP.V1_UP	136	Lenalidomide resistance	Neri[19]	1.44	.005	0.206	1.00	.452	0.486
RAF_UP.V1_DN	183	Lenalidomide resistance	Neri[19]		NE		1.12	.181	0.358
MEK_UP.V1_DN	182	Lenalidomide resistance	Neri[19]		NE		1.03	.388	0.445
RPS14_DN.V1_DN	179	Lenalidomide resistance	Neri[19]	1.12	.109	0.333		NE	
AKT_UP_MTOR_DN.V1_DN	173	Lenalidomide resistance	Neri[19]		NE		1.12	.217	0.334
STK33_DN	256	Lenalidomide resistance	Neri[19]		NE		1.33	.004	0.103

Abbreviations: ATL, adult T-cell leukemia/lymphoma; FDR, false discovery rate; KEGG, Kyoto Encyclopedia of Genes and Genomes; NE, not enriched; NES, normalized enrichment score; TTD, Therapeutic Target Database.

treatment. Overall survival has not been shown to benefit from aggressive intervention with cytotoxic agents because of serious treatment-associated toxicities, including prolonged myelosuppression. An increased understanding of the pathogenesis of SS, with the identification of new targets, has led to new therapeutic approaches with biologic agents to reduce treatment-related toxicities and improve outcomes.[1]

The rationale for lenalidomide selection by the MTB was based on five factors. First, lenalidomide binds the cullin 4-RING-E3 ubiquitin ligase cereblon complex and degrades lymphoid transcription factors IKZF1 and IKZF3, leading to a decrease in NF-κB.[12] Second, activated tumor necrosis factor signaling, known as a lenalidomide-target pathway in the KEGG DRUG database, was detected in the tumor, which is also considered targetable by lenalidomide on the basis of our in-house data, UPN1. Third, a phase II trial of lenalidomide monotherapy for advanced refractory CTCL reported reliable and meaningful clinical benefits; in that trial, lenalidomide-induced TFR was correlated with good clinical response in patients with SS, which suggests that mechanisms that underlie this reaction might represent specific anticancer immune responses.[9] Indeed, in the current patient, immune response to cancer was considered to be induced by lenalidomide as shown by the appearance of TFR (Fig 1C). Immunohistochemical staining showed that $CD8^+$ cells in the tumor after the appearance of TFR were increased after lenalidomide treatment. Fourth, lenalidomide exerts immunomodulatory effects, such as NK- and T-cell activation and the induction of T-helper 1 cytokine production and cytotoxic activity; it also alters the tumor microenvironment through its anti-angiogenic, antiproliferative, and pro-apoptotic properties.[13] These characteristics provided the rationale for using this agent in our elderly patient with SS with susceptibility to infection. Actually, NK-cell–mediated cytotoxicity and cytokine-cytokine receptor interactions were enriched in the tumor before lenalidomide treatment. In addition, the frequencies of circulating NK cells and $CD3^+CD8^+$ T cells increased after the administration of lenalidomide compared

FIG 1. Changes in the patient's skin lesions during lenalidomide treatment. (A) The skin lesions on the trunk and arms before lenalidomide treatment. (B) After the first treatment course, almost all skin lesions except for that on the patient's sternal region disappeared. (C) Documented transient flare reaction presented as erythema around skin lesions. (D) All lesions, including the sternal lesion, disappeared after the fifth cycle.

with those at first treatment (Appendix Fig A11). In contrast, the frequency of effector regulatory T cells did not increase (Appendix Fig A11). These findings were similar to those described in the immunohistochemistry (Appendix Fig A6). These immunologic changes might have induced anticancer effects[9] and prevented severe infection.[14] Finally, the Japanese national health insurance system has already approved lenalidomide for the treatment of myelodysplastic syndrome, refractory/relapse multiple myeloma, and ATL.

Lenalidomide did not adequately treat the patient's bulky sternal mass. Acquired lenalidomide resistance is considered to be caused by reduced levels of tumor cell cereblon protein because of epigenetic modifications of the cereblon promotor region, cereblon gene mutations or chromosomal deletions, or acquired cereblon pathway mutations and detects in other components of the E3 ligase complex.[15] Another possible reason is that the delivery of lenalidomide to the tumor was hindered by the abundant surrounding interstitial tissue and the immunosuppressive tumor microenvironment.[16]

In the near future, clinical sequencing will support clinical decisions with regard to appropriate treatments for patients with rare and refractory cancers. In addition, clinical sequencing on the basis of a combination of several NGS techniques might be particularly useful in identifying appropriate treatment options. This case report is the first to our knowledge of the use of clinical sequencing to identify a successful treatment strategy for a patient with refractory SS.

AFFILIATIONS

[1]Department of General Medicine, IMSUT Hospital, Institute of Medical Science, The University of Tokyo, Tokyo, Japan
[2]Department of Hematology/Oncology, IMSUT Hospital, Institute of Medical Science, The University of Tokyo, Tokyo, Japan
[3]Department of Applied Genomics, Research Hospital, Institute of Medical Science, The University of Tokyo, Tokyo, Japan
[4]Laboratory of DNA Information Analysis, Human Genome Center, Institute of Medical Science, The University of Tokyo, Tokyo, Japan
[5]Laboratory of Tumor Cell Biology, Department of Computational Biology and Medical Sciences, Graduate School of Frontier Sciences, The University of Tokyo, Tokyo, Japan
[6]Division of Molecular Therapy, Advanced Clinical Research Center, Institute of Medical Science, The University of Tokyo, Tokyo, Japan
[7]Department of Diagnostic Pathology, IMSUT Hospital, Institute of Medical Science, The University of Tokyo, Tokyo, Japan
[8]Division of Health Medical Data Science, Health Intelligence Center, Institute of Medical Science, The University of Tokyo, Tokyo, Japan

CORRESPONDING AUTHOR

Arinobu Tojo, MD, PhD, Institute of Medical Science, The University of Tokyo, 4-6-1 Shirokanedai, Minato-ku, Tokyo 108-8639, Japan; e-mail: a-tojo@ims.u-tokyo.ac.jp.

EQUAL CONTRIBUTION

Y.H. and K.Y. contributed equally as co-first authors.
K.Y. and A.T. contributed equally as senior authors.

SUPPORT

Supported in part by the Center of Innovation Program of the Japan Science and Technology Agency and Ministry of Education, Culture, Sports, Science and Technology Innovative Area 15H05912.

AUTHOR CONTRIBUTIONS

Conception and design: Kazuaki Yokoyama, Arinobu Tojo
Financial support: Kenzaburo Tani, Satoru Miyano
Administrative support: Hiroshi Yotsuyanagi
Provision of study material or patients: Makoto Nakashima, Yasunori Ota, Kaoru Uchimaru
Collection and assembly of data: Yasuki Hijikata, Kazuaki Yokoyama, Makoto Yamagishi, Lay Ahyoung Lim, Kaoru Uchimaru
Data analysis and interpretation: Yasuki Hijikata, Kazuaki Yokoyama, Nozomi Yokoyama, Yasuo Matsubara, Eigo Shimizu, Makoto Nakashima, Yasunori Ota, Rui Yamaguchi, Mika Ito, Yukihisa Tanaka, Tamami Denda, Kenzaburo Tani, Hiroshi Yotsuyanagi, Seiya Imoto, Satoru Miyano
Manuscript writing: All authors
Final approval of manuscript: All authors
Accountable for all aspects of the work: All authors

DATA AVAILABILITY STATEMENT

Both sequence data and materials described in this article are available upon request to the corresponding author K.Y. (k-yoko@ims.u-tokyo.ac.jp), but the request must include a description of the research proposal.

AUTHORS' DISCLOSURES OF POTENTIAL CONFLICTS OF INTEREST

The following represents disclosure information provided by authors of this manuscript. All relationships are considered compensated unless otherwise noted. Relationships are self-held unless noted. I = Immediate Family Member, Inst = My Institution. Relationships may not relate to the subject matter of this manuscript. For more information about ASCO's conflict of interest policy, please refer to www.asco.org/rwc or ascopubs.org/po/author-center.

Open Payments is a public database containing information reported by companies about payments made to US-licensed physicians (Open Payments).

Rui Yamaguchi
Honoraria: Janssen Pharmaceuticals, Chugai Pharma

Kenzaburo Tani
Stock and Other Ownership Interests: Shinnihonseiyaku Co Ltd, Precision Therapeutics, Oncolys BioPharma
Consulting or Advisory Role: Precision Therapeutics
Research Funding: Shinnihonseiyaku Co Ltd, Neopharma Japan, Takara Bio

Kaoru Uchimaru
Honoraria: Celgene
Research Funding: Daiichi Sankyo, Celgene, NEC

Arinobu Tojo
Honoraria: Otsuka Pharmaceutical
Consulting or Advisory Role: Sysmex
Speakers' Bureau: Novartis, Otsuka Pharmaceutical, Bristol-Myers Squibb
Research Funding: Chugai Pharma, Torii Pharmaceutical, KM Biologics

No other potential conflicts of interest were reported.

ACKNOWLEDGMENT

We thank all members of the study team as well as the patients and their families.

REFERENCES

1. Agar NS, Wedgeworth E, Crichton S, et al: Survival outcomes and prognostic factors in mycosis fungoides/Sézary syndrome: Validation of the revised International Society for Cutaneous Lymphomas/European Organisation for Research and Treatment of Cancer staging proposal. J Clin Oncol 28:4730-4739, 2010
2. Wilcox RA: Cutaneous T-cell lymphoma: 2017 update on diagnosis, risk-stratification, and management. Am J Hematol 92:1085-1102, 2017
3. Wang L, Ni X, Covington KR, et al: Genomic profiling of Sézary syndrome identifies alterations of key T cell signaling and differentiation genes. Nat Genet 47:1426-1434, 2015
4. Wakai T, Prasoon P, Hirose Y, et al: Next-generation sequencing-based clinical sequencing: Toward precision medicine in solid tumors. Int J Clin Oncol 24:115-122, 2019
5. Patel NM, Michelini VV, Snell JM, et al: Enhancing next-generation sequencing-guided cancer care through cognitive computing. Oncologist 23:179-185, 2018
6. KEGG: Kyoto Encyclopedia of Genes and Genomes. http://www.kegg.jp or http://www.genome.jp/kegg
7. Kyoto Encyclopedia of Genes and Genomes: KEGG DRUG: Lenalidomide. https://www.kegg.jp/dbget-bin/www_bget?D04687+-us
8. Innovative Drug Research and Bioinformatics Group: Therapeutic Target Database. http://db.idrblab.net/ttd/data/drug/details/d0q5nx
9. Querfeld C, Rosen ST, Guitart J, et al: Results of an open-label multicenter phase 2 trial of lenalidomide monotherapy in refractory mycosis fungoides and Sézary syndrome. Blood 123:1159-1166, 2014
10. Bagot M, Hasan B, Whittaker S, et al: A phase III study of lenalidomide maintenance after debulking therapy in patients with advanced cutaneous T-cell lymphoma - EORTC 21081 (NCT01098656): Results and lessons learned for future trial designs. Eur J Dermatol 27:286-294, 2017
11. Damodaran S, Berger MF, Roychowdhury S: Clinical tumor sequencing: Opportunities and challenges for precision cancer medicine. Am Soc Clin Oncol Educ Book 35:e175-e182, 2015
12. Kritharis A, Coyle M, Sharma J, et al: Lenalidomide in non-Hodgkin lymphoma: Biological perspectives and therapeutic opportunities. Blood 125:2471-2476, 2015
13. Kotla V, Goel S, Nischal S, et al: Mechanism of action of lenalidomide in hematological malignancies. J Hematol Oncol 2:36, 2009
14. Lenartić M, Jelenčić V, Zafirova B, et al: NKG2D promotes B1a cell development and protection against bacterial infection. J Immunol 198:1531-1542, 2017
15. Franssen LE, Nijhof IS, Couto S, et al: Cereblon loss and up-regulation of c-Myc are associated with lenalidomide resistance in multiple myeloma patients. Haematologica 103:e368-e371, 2018
16. Sriraman SK, Aryasomayajula B, Torchilin VP: Barriers to drug delivery in solid tumors. Tissue Barriers 2:e29528, 2014
17. Aue G, Sun C, Liu D, et al: Activation of Th1 immunity within the tumor microenvironment is associated with clinical response to lenalidomide in chronic lymphocytic leukemia. J Immunol 201:1967-1974, 2018

18. Bhutani M, Zhang Q, Friend R, et al: Investigation of a gene signature to predict a gene signature to predict response to immunomodulatory derivatives for patients with multiple myeloma: An exploratory, retrospective study using microarray datasets from prospective clinical trials. Lancet Haematol 4:e443-e451, 2017

19. Neri P, Gratton K, Ren L, et al: RNA-sequencing of paired pre-treatment and relapse samples reveals differentially expressed genes associated with lenalidomide resistance in multiple myeloma. Blood 122:530, 2013

APPENDIX

Materials and Methods

Patients and samples. Our study protocol was approved by our institutional research ethics committee and was in accordance with the Declaration of Helsinki. Three patients were recruited for our study, all of whom provided written informed consent. The characteristics of two reference patients with adult T-cell leukemia/lymphoma (ATL) are listed in Table A2. The following samples were collected: (1) the tumor (cutaneous T-cell lymphoma [CTCL]), patient's skin tumor sample before lenalidomide therapy, and control (CTCL), patient's tumor-free normal skin lesion, which had been histologically confirmed, and (2) the tumor (ATL), tumor-rich peripheral blood mononuclear cells (PBMNCs) before lenalidomide therapy in a patient with ATL(unique patient number 1 [UPN1]) for whom clinical partial response was observed under lenalidomide therapy, and control (ATL), tumor-rich PBMNCs before lenalidomide therapy in another patient with ATL (UPN2) for whom no objective response had been observed with lenalidomide therapy.

Extraction of DNA and RNA. DNA was extracted using the Gentra Puregene Blood Kit and the QIAamp Circulating Nucleic Acid Kit (QIAGEN, Hilden, Germany). DNA was quantified using the Qubit dsDNA HS Assay Kit (Life Technologies, Carlsbad, CA). Total RNA was extracted using the RNeasy Mini Kit (QIAGEN).

Whole-exome sequencing. To identify driver mutations, we performed whole-exome sequencing (WES). Libraries were prepared from 200 ng of paired DNA (tumor/control) using SureSelectXT Human All Exon V5 (Agilent Technologies, Santa Clara, CA). WES was performed on the basis of 2 × 100-base pair (bp) paired-end reads on the NextSeq 500 platform with NextSeq 500/550 Kit v2 chemistry (Illumina, San Diego, CA). All procedures were performed according to the manufacturers' protocols.

Somatic variant calling and subsequent primary filtering of WES data. We used human genome build 19 as the reference sequence for our analysis. Primary processing of sequencing data was performed using our in-house software. Single nucleotide variants were identified using Genomon2 (http://genomon.hgc.jp/exome/en/) with default parameters. All variant calls were annotated with ANNOVAR (using an in-house annotation database resource). The Integrative Genomics Viewer (IGV) version 2.3.57 (https://software.broadinstitute.org/software/igv/download) was used to visualize and inspect the read alignments and variant calls. For our analysis, the databases used to annotate variants included the following: RefSeq (http://www.ncbi.nlm.nih.gov/RefSeq/), the 1000 Genomes Project as of August 2015 (http://www.internationalgenome.org/data), dbSNP131 (http://www.ncbi.nlm.nih.gov/projects/SNP/), ToMMo version 1 (https://ijgvd.megabank.tohoku.ac.jp/), the Human Genetic Variation Database as of October 2013 (http://www.hgvd.genome.med.kyoto-u.ac.jp/), ClinVar as of June 2015 (https://www.ncbi.nlm.nih.gov/clinvar/), the Human Gene Mutation Database Professional as of March 2015 (http://www.hgmd.cf.ac.uk/ac/index.php), the cBioPortal for Cancer Genomics as of September 2015 (http://cbioportal.org), the TumorPortal as of September 2015 (http://www.tumorportal.org/), the Catalogue of Somatic Mutations in Cancer (COSMIC) version 70 (http://cancer.sanger.ac.uk/cosmic), and the International Cancer Genome Consortium Data Portal (https://dcc.icgc.org/). The computational algorithms Sorting Intolerant From Tolerant (http://sift-dna.org) and PolyPhen-2 (http://genetics.bwh.harvard.edu/pph2/) were used to predict whether mutations were damaging. Synonymous or noncoding variants were excluded, and single nucleotide polymorphisms (SNPs; minor allele frequency > 1%) reported to be present in either of the aforementioned SNP databases were automatically excluded, unless they were recurrently (three or more times) found in the COSMIC database. Copy number variation analysis was performed using CNVkit version 0.8.2 software (E. Talevich, University of Southern California, San Francisco, San Francisco, CA), and the data were filtered on the basis of the following parameters: $\log_2 \geq 0.6$ or $\log_2 \leq -1$ and read depth > 10. Upon somatic mutation calling followed by a primary filtering step, the list of variants was stored in a variant calling file format (.vcf). Gene-level copy number alterations, as a $\log_2$ ratio of tumor to normal, were also stored in text format (.log2).

Identification of putative driver mutations from WES data. We classified variants into three tiers. We regarded tier 1 mutations as definitive driver mutations. Briefly, tier 1 included definitive driver mutations with abundant evidence in the literature and/or cancer mutation databases with a variant frequency (VAF) of ≥ 5%. Tier 2 included mutations with a little or no evidence in the literature and/or databases, namely, uncertain/unclassified significance, with VAF ≥ 5%. Tier 3 included all remaining variants. The selection of mutation criteria for tier 1 was as follows: all changes in the amino acid coding regions of annotated exons that were frequently (at least three times) reported in hematopoietic tumor samples in the COSMIC database (version 71) or all predictive, highly deleterious variants (in consensus splice site regions, frameshift mutations, any premature predicted truncation mutation, or large in-frame insertions/deletions) in non-Hodgkin lymphoma or CTCL-associated genes, according to previous studies (Ungewickell A, et al: Nat Genet 47:1056-1060, 2015; Choi J, et al: Nat Genet 47:1011-1019, 2015; Lohr JG, et al: Proc Natl Acad Sci U S A 109:3879-3884, 2012). Curated tier 1-2 somatic mutations are listed in Table A1.

RNA Sequencing

We used the following RNA samples: the tumor (CTCL), patient's skin tumor sample before lenalidomide therapy; control (CTCL), and patient's tumor-free normal skin lesion; the tumor (ATL) and tumor-rich PBMNCs in lenalidomide-responsive ATL (UPN1); and the control (ATL) and tumor-rich PBMNCs in lenalidomide-primary refractory ATL (UPN2). cDNA libraries for next-generation sequencing were constructed from 100 ng of total RNA using TruSeq RNA Access Library Prep Kit (Illumina). Each paired end–indexed library was sequenced to a length of 75 nucleotides per pair (2 × 75 bp) using a NextSeq instrument. Sequence reads were processed by our in-house Genomon-RNA/Genomon-expression pipeline (Shiraishi Y, et al: PLoS One 9: e114263, 2014; http://genomon.hgc.jp/rna/). IGV version 2.3.57 was used to visualize the mapped sequence. For gene expression, fragments per kilobase of gene model per million mapped read (FPKM) values were calculated and used.

To investigate any changes in gene expression in a certain enriched pathway involved in the clinical features of the current patient with CTCL, as well as the reference patients with ATL, we used the online DAVID tool version 6.8 (https://david.ncifcrf.gov/) and gene set enrichment analysis (GSEA) with FPKM metrics at the gene level (tumor *v* control). For DAVID-based pathway analysis, upregulated genes relative to expression in the control (fold-change ≥ 2 and with a cutoff value of FPKM ≥ 10) were stored in comma-separated value format (.csv) and inputted into the web-based interface of DAVID. These outputs were reviewed, and significantly enriched Kyoto Encyclopedia of Genes and Genomes (KEGG) pathways are listed in Table A3. The four significant lenalidomide-target pathways were also visualized using Pathview (https://pathview.uncc.edu/) and displayed in Figures A7-A10. For GSEA, a stand-alone application was used (Broad Institute, Cambridge, MA; http://broadinstitute.org/gsea/index.jsp) with the MSIGDB library version 7.1 as well as in-house–created gene sets that were based on a false discovery rate threshold of $q < 0.05$.

Immunohistochemistry

Formalin-fixed paraffin embedded tissue sections of 3-μm thickness were deparaffinized in xylene and rehydrated in a series of graded alcohols and heated in an antigen retrieval solution at pH 9.0 (Vector Laboratories, Burlingame, CA) for 10 minutes at 120°C. Endogenous peroxidase was blocked by incubation with 3% hydrogen peroxidase for 5 minutes at room temperature. Next, sections were incubated with the following primary antibodies for 30 minutes at 37°C: CD4 (clone EPR6855, dilution 1:250; Abcam, Cambridge, United Kingdom), CD8 (clone SP16, dilution 1:100;

Abcam), CD25 (clone 305, dilution 1:80; Leica Biosystems, Newcastle, United Kingdom), and Foxp3 (clone SP97, dilution 1:80; Abcam). After washing, sections were treated with secondary antibody (EnVision+ Dual Link System-HRP; Dako, Glostrup, Denmark) for 30 minutes at 37°C. To visualize antigen-antibody complex, EnVision+ DAB kit (Dako) was used, and then sections were counterstained in hematoxylin. Normal lymph node was placed on the same slide glass as a positive control, and negative controls were used in phosphate-buffered saline instead of the primary antibodies.

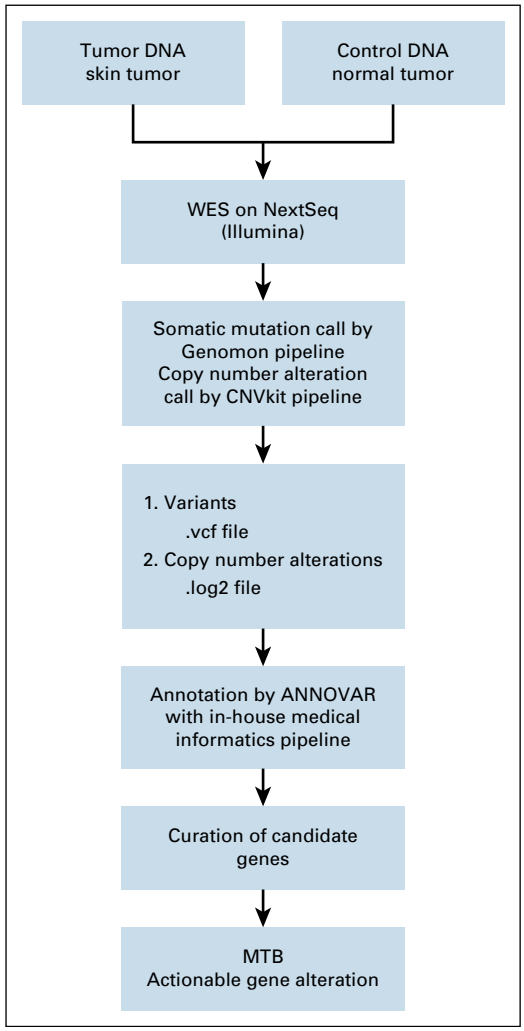

FIG A1. Flowchart of whole-exome sequencing. MTB, molecular tumor board; vcf, variant calling file; WES, whole exome sequencing.

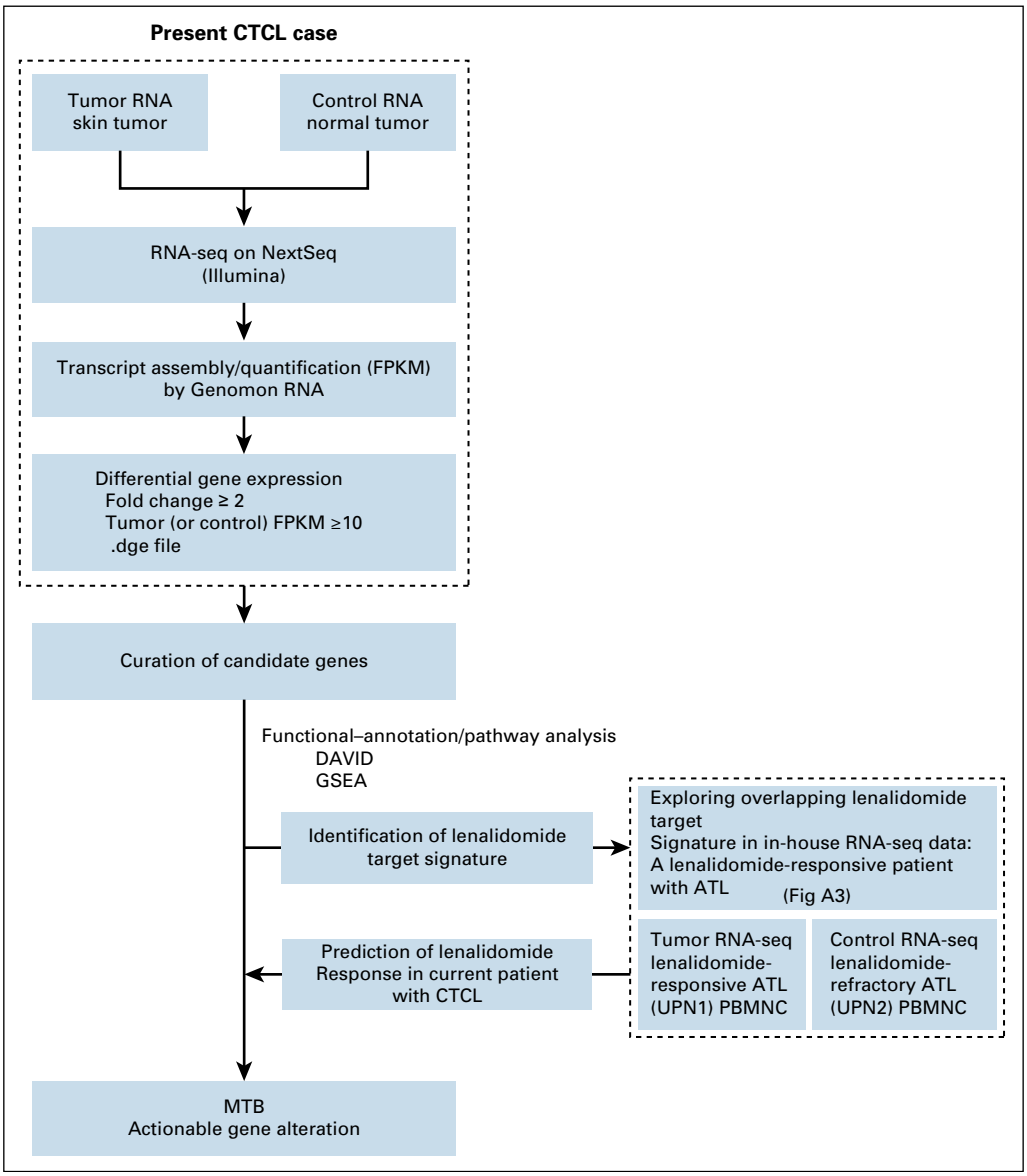

FIG A2. Flow of overall RNA sequencing. ATL, adult T-cell leukemia/lymphoma; CTCL, cutaneous T-cell lymphoma; .dge, digital gene expression; FPKM, fragments per kilobase of gene model per million mapped read; GSEA, gene set enrichment analysis; Len, lenalidomide; MTB, molecular tumor board; PBMNC, peripheral blood mononuclear cell; RNA-seq, RNA sequencing; UPN, unique patient number.

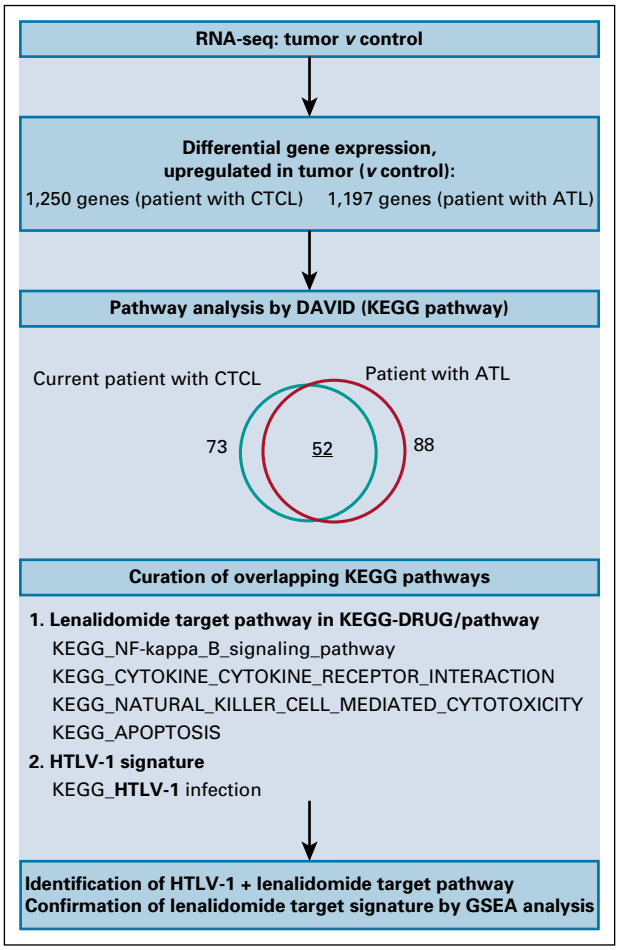

FIG A3. Flow chart of overlapping lenalidomide (Len) target signature discovery. ATL, adult T-cell leukemia/lymphoma; CTCL, cutaneous T-cell lymphoma; GSEA, gene set enrichment analysis; KEGG, Kyoto Encyclopedia of Genes and Genomes; RNA-seq, RNA sequencing.

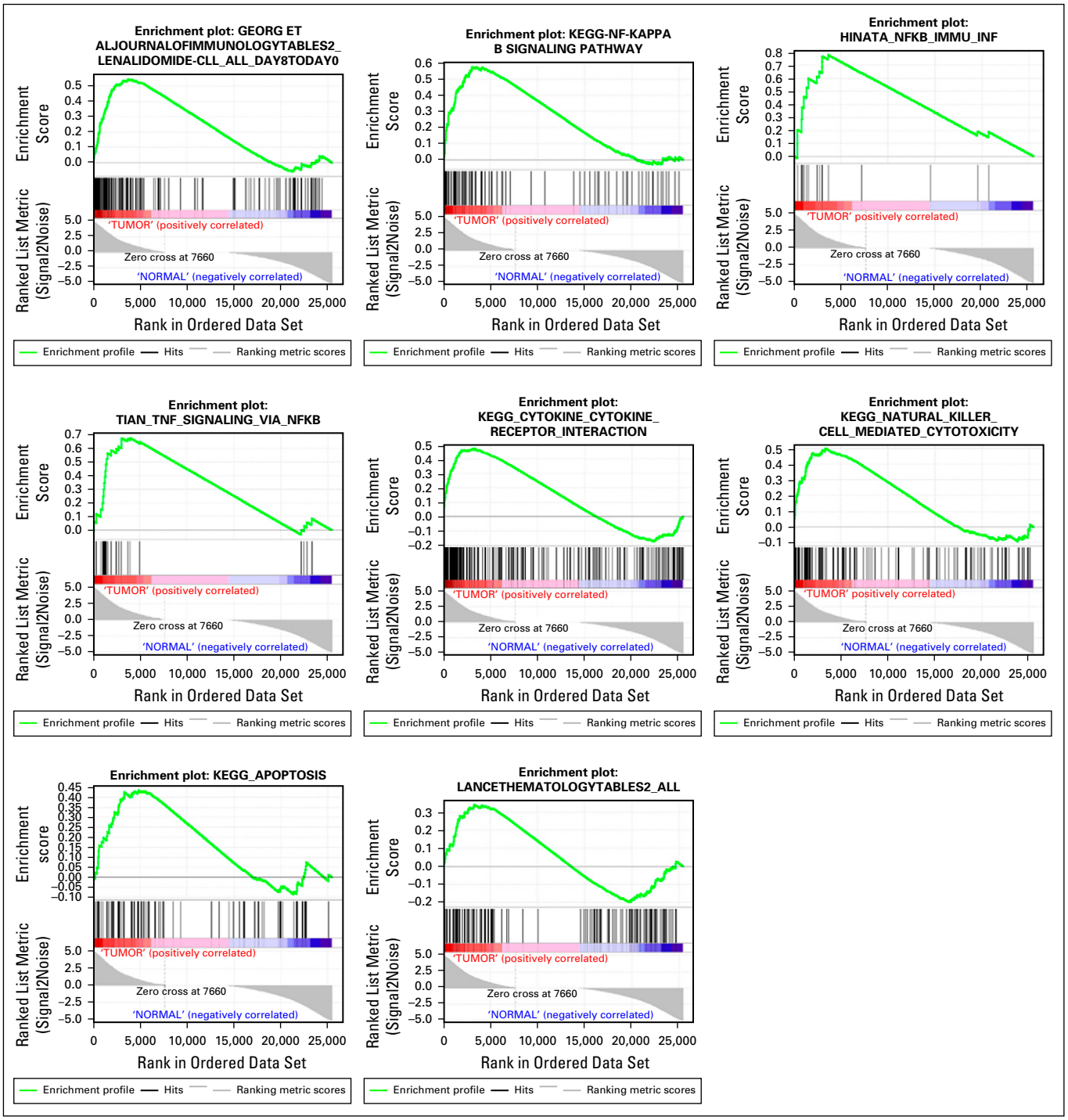

FIG A4. Lenalidomide-target signature enriched in cutaneous T-cell lymphoma (CTCL) on the basis of gene set enrichment analysis (GSEA; related to Table 1). Enrichment plots and heat maps from GSEA in the patient. GSEA of the tumor disclosed significant enrichment of nuclear factor-κB (NF-κB) pathways, including that of a custom gene set, GEORG ETALJOURNALOFIMMUNOLOGYTABLES2_LENALIDOMIDE-CLL_ALL_DAY8TODAY0, on the basis of the report and Supplementary Table 2 by Aue et al[17] as follows: NATURAL_KILLER_CELL_MEDIATED_CYTOTOXICITY from the MSIGDB library, CYTOKINE_CYTOKINE_RECEPTOR_INTERACTION from the MSIGDB library, TIAN_TNF_SIGNALING_VIA_NFKB and APOPTOSIS from the MSIGDB library, and a custom gene set, LANCETHEMATOLOGYTABLES2_ALL, on the basis of the report and Supplementary Table 2 by Bhutani et al[18]. Red indicates that gene expression increased compared with that in control. Blue indicates that gene expression decreased compared with that in control. KEGG, Kyoto Encyclopedia of Genes and Genomes.

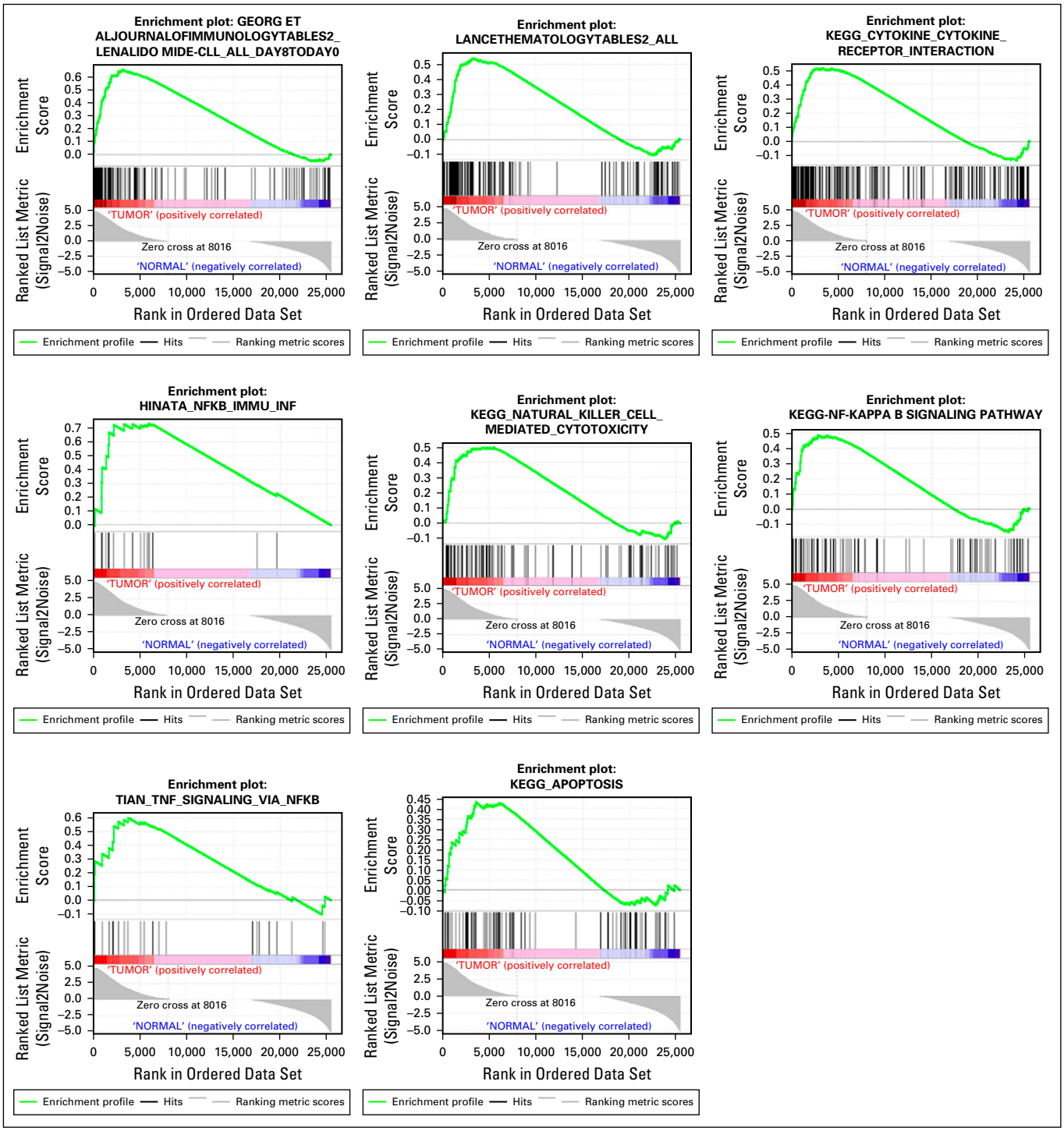

FIG A5. Lenalidomide-target signature enriched in adult T-cell leukemia/lymphoma (ATL) on the basis of gene set enrichment analysis (GSEA; related to Table 1). Enrichment plots and heat maps from GSEA of ATL. In relation to Fig A4, GSEA of the tumor disclosed significant enrichment of nuclear factor-κB (NF-κB) pathways, including the gene sets of NATURAL_KILLER_CELL_MEDIATED_CYTOTOXICITY, CYTOKINE_CYTOKINE_RECEPTOR_INTERACTION, TIAN_TNF_SIGNALING_VIA_NFKB, APOPTOSIS and custom gene sets on the basis of the report and Appendix Table A2 by Aue et al[17] and Bhutani et al[18]. Red indicates that gene expression increased compared with that in the control. Blue indicates that gene expression decreased compared with that in the control. KEGG, Kyoto Encyclopedia of Genes and Genomes.

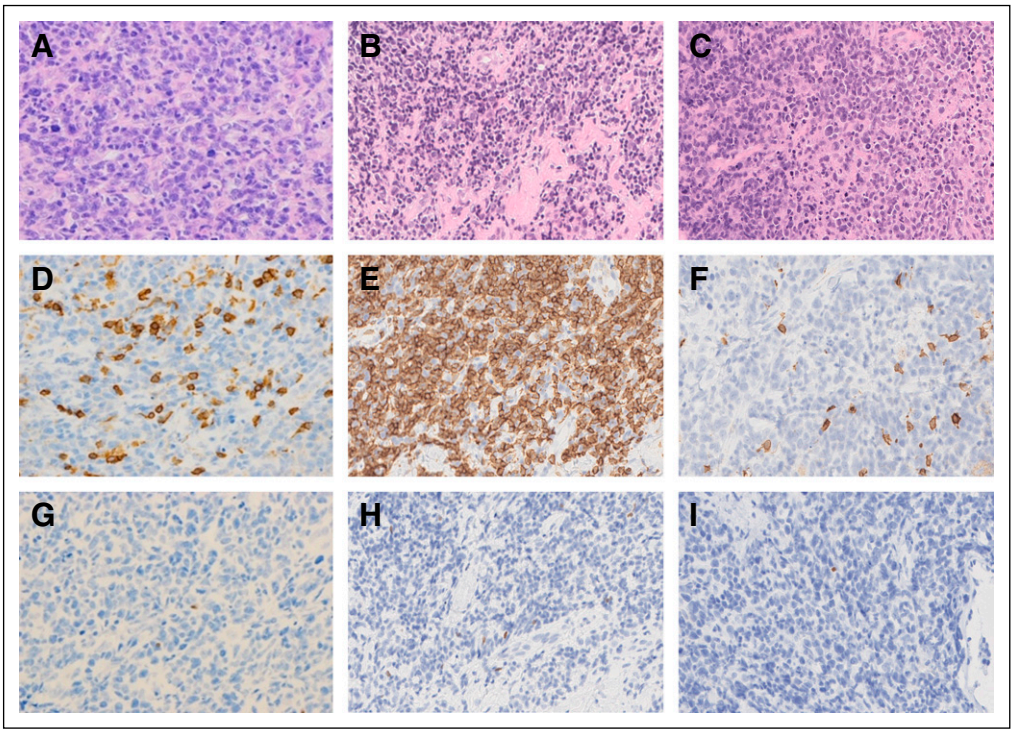

FIG A6. Histologic and immunohistochemical analysis of tumor specimens before and after the lenalidomide treatment. Hematoxylin and eosin staining and anti-CD8 and anti-Foxp3 antibody staining of tumor cells and lymphocytes (A, D, and G) before the lenalidomide treatment, (B, E, and H) in a tumor showing good response after the first course, and (C, F, and I) in a tumor showing a poor response after three courses of lenalidomide. (D and E) A remarkable number of $CD8^+$ cells are shown, whereas (G, H, and I) few $Foxp3^+$ cells were observed in each tumor. The number of $CD8^+$ cells after the first course of lenalidomide was increased compared with that (E) before treatment but was decreased in the poorly responding lesion (F) after the third course of lenalidomide.

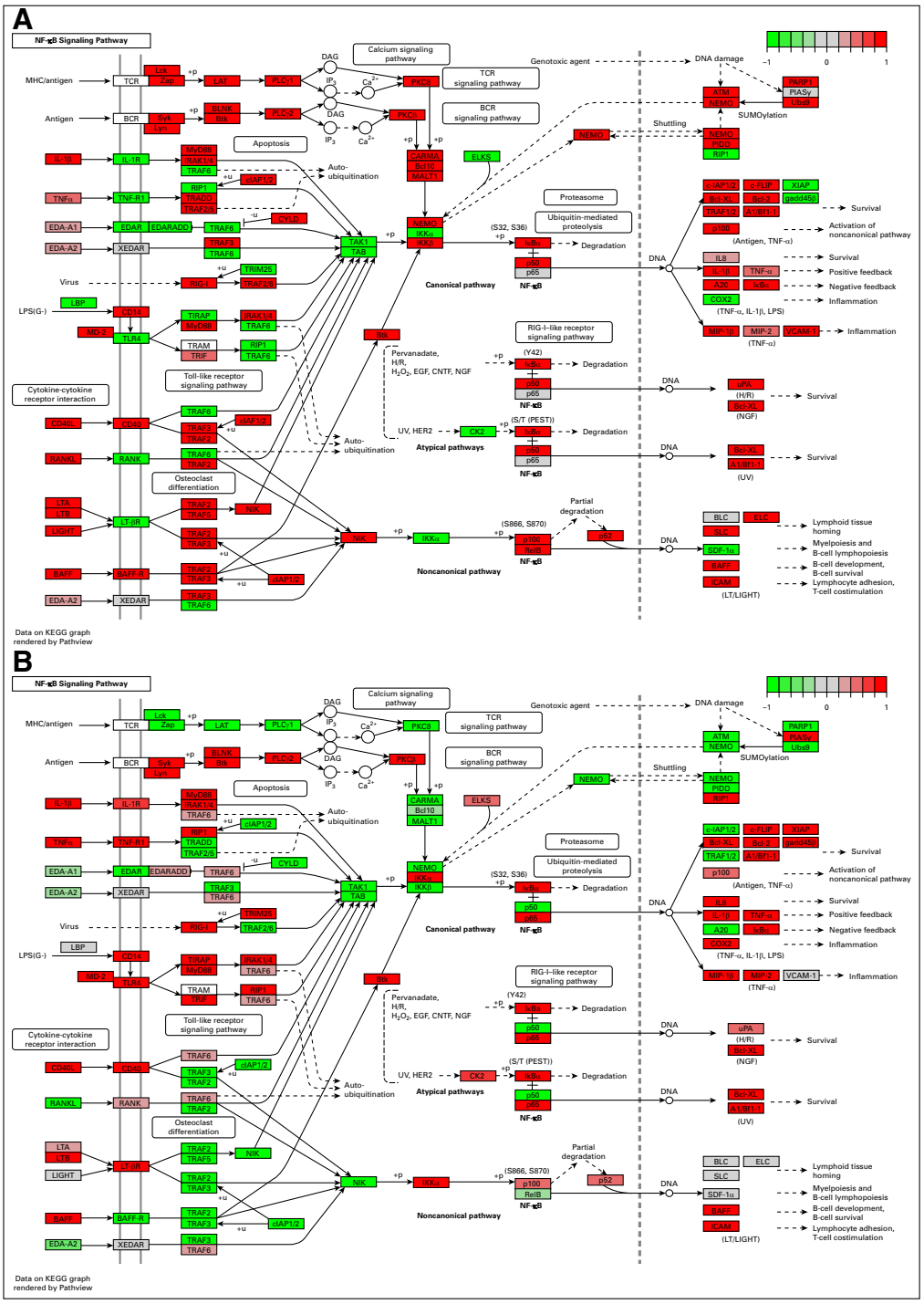

FIG A7. Lenalidomide target pathway: nuclear factor-κB (NF-κB) signaling pathway. (A) Cutaneous T-cell lymphoma. (B) Adult T-cell leukemia/lymphoma. Green gradient colors indicate downregulation of the gene, and red colors indicate upregulation of the gene relative to the control sample. BCR, B-cell receptor; H/R, hypoxia/reoxygenation; IL, interleukin; KEGG, Kyoto Encyclopedia of Genes and Genomes; LPS, lipopolysaccharide; MHC, major histocompatibility complex; TCR, T-cell receptor; TNF-α, tumor necrosis factor-α; UV, ultraviolet.

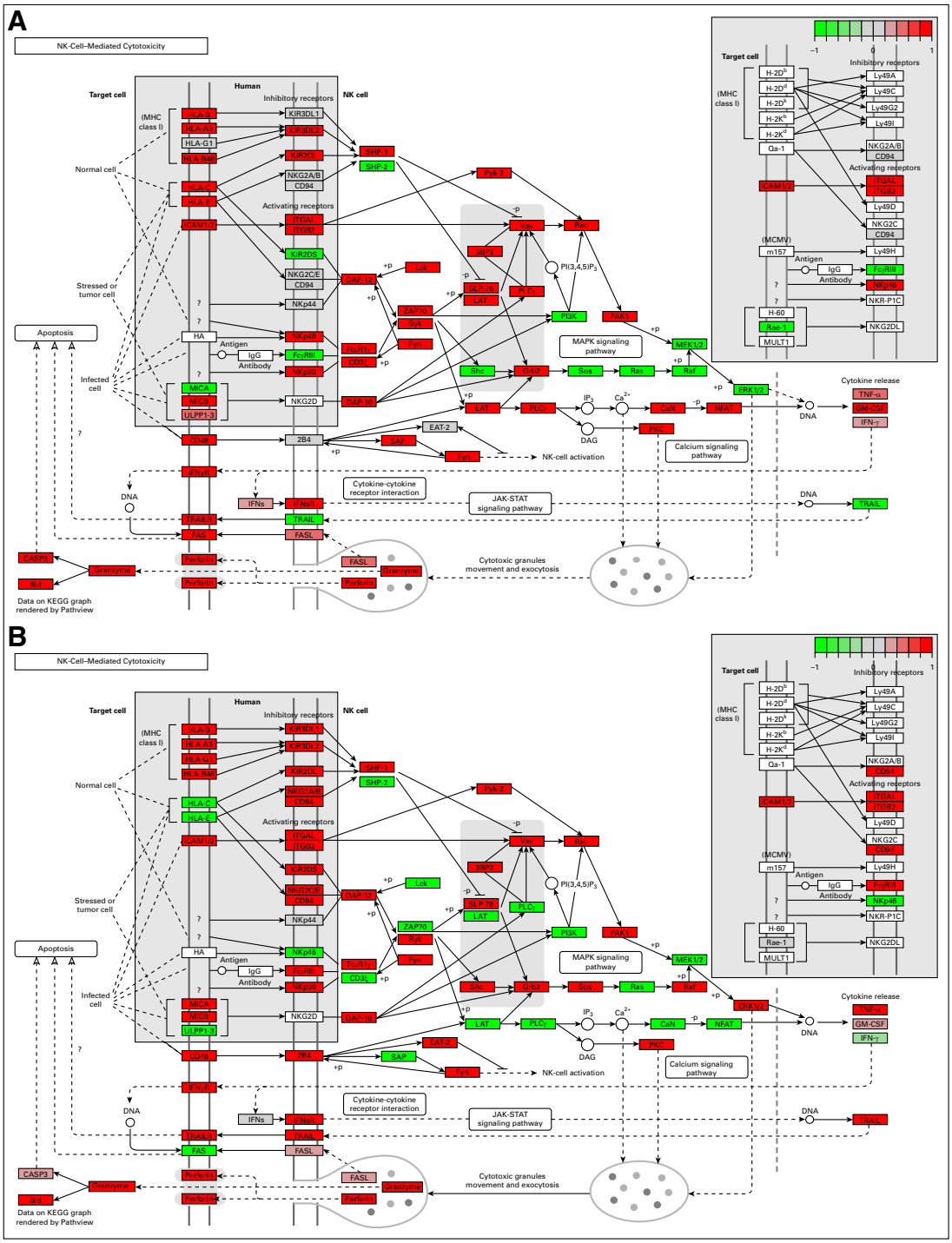

FIG A8. Lenalidomide target pathway: natural killer (NK)-cell–mediated cytotoxicity. (A) Cutaneous T-cell lymphoma. (B) Adult T-cell leukemia/lymphoma. Green gradient colors indicate downregulation of the gene, and red colors indicate upregulation of the gene relative to the control sample. JAK-STAT, Janus kinase–signal transducers and activators of transcription; KEGG, Kyoto Encyclopedia of genes and genomes; MAPK, mitogen-activated protein kinase; MCMV, murine cytomegalovirus; MHC, major histocompatibility complex.

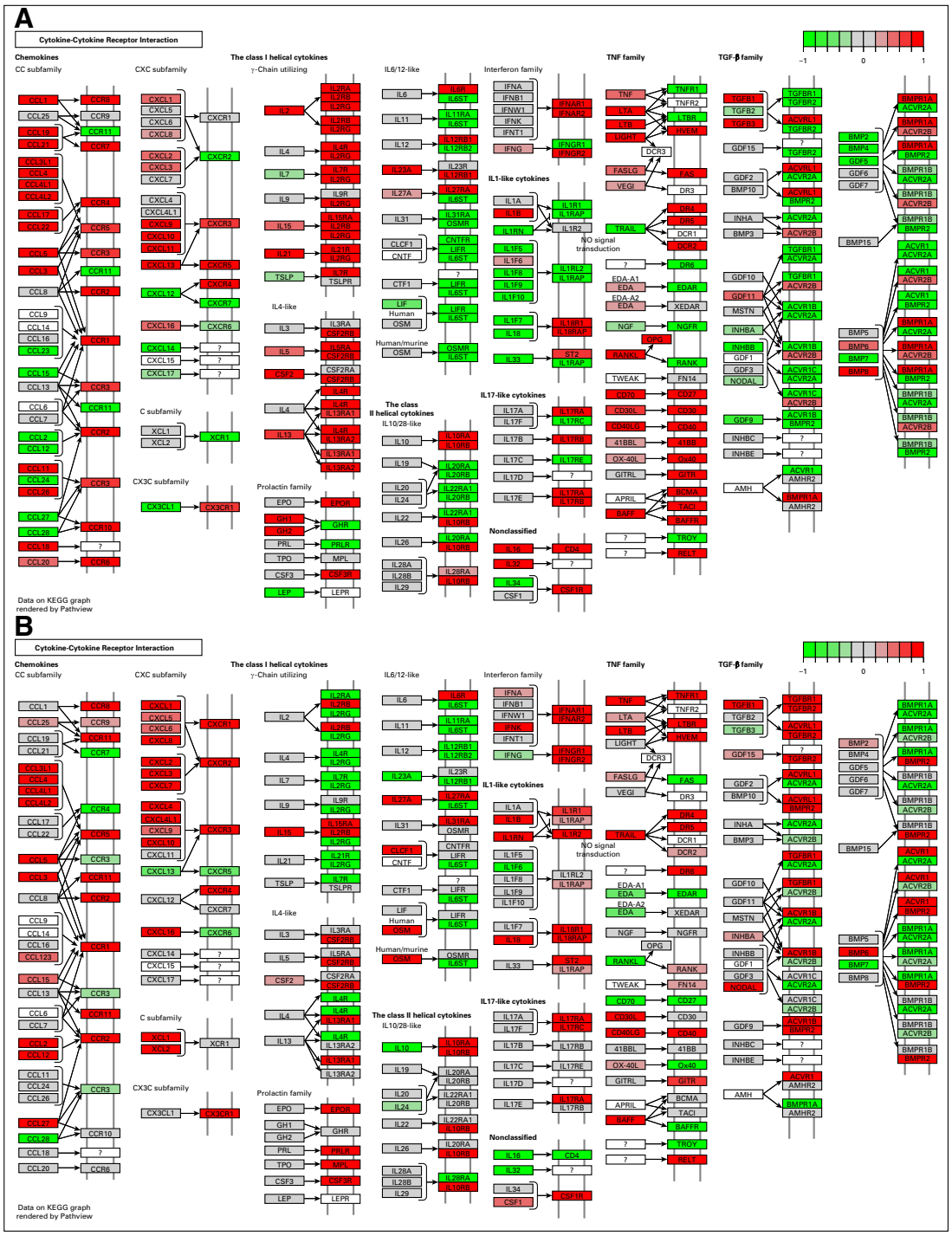

FIG A9. Lenalidomide target pathway: cytokine-cytokine receptor interaction. (A) Cutaneous T-cell lymphoma. (B) Adult T-cell leukemia/lymphoma. Green gradient colors indicate downregulation of the gene, and red colors indicate upregulation of the gene relative to the control sample. IFN, interferon; IL, interleukin; KEGG, Kyoto Encyclopedia of genes and genomes; TGF-β, transforming growth factor-β; TNF, tumor necrosis factor.

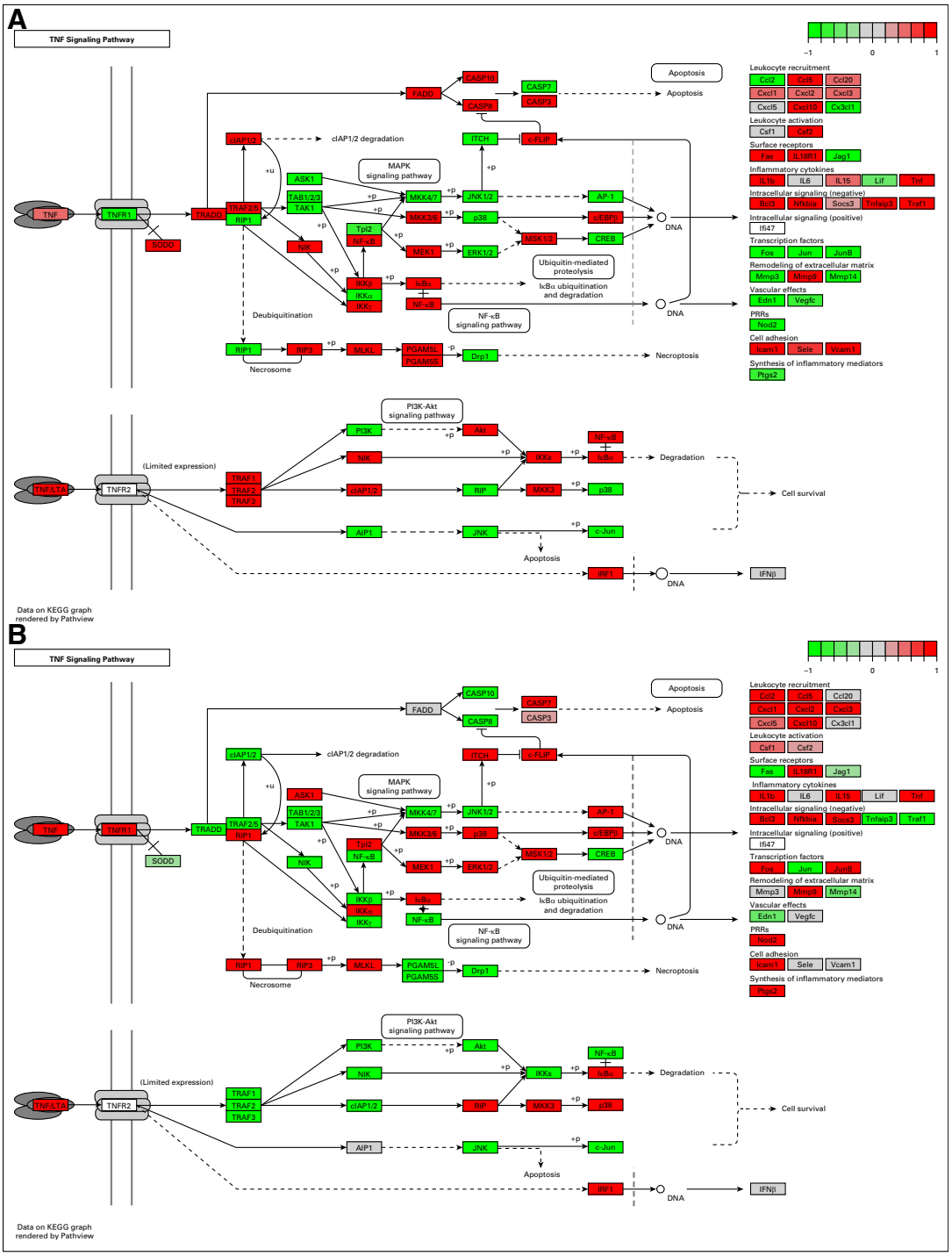

FIG A10. Lenalidomide target pathway: tumor necrosis factor (TNF) signaling pathway. (A) Cutaneous T-cell lymphoma. (B) Adult T-cell leukemia/lymphoma. Green gradient colors indicate downregulation of the gene, and red colors indicate upregulation of the gene relative to the control sample. KEGG, Kyoto Encyclopedia of genes and genomes; MAPK, mitogen-activated protein kinase; NF-κB, nuclear factor-κB; PRR, pattern recognition receptor.

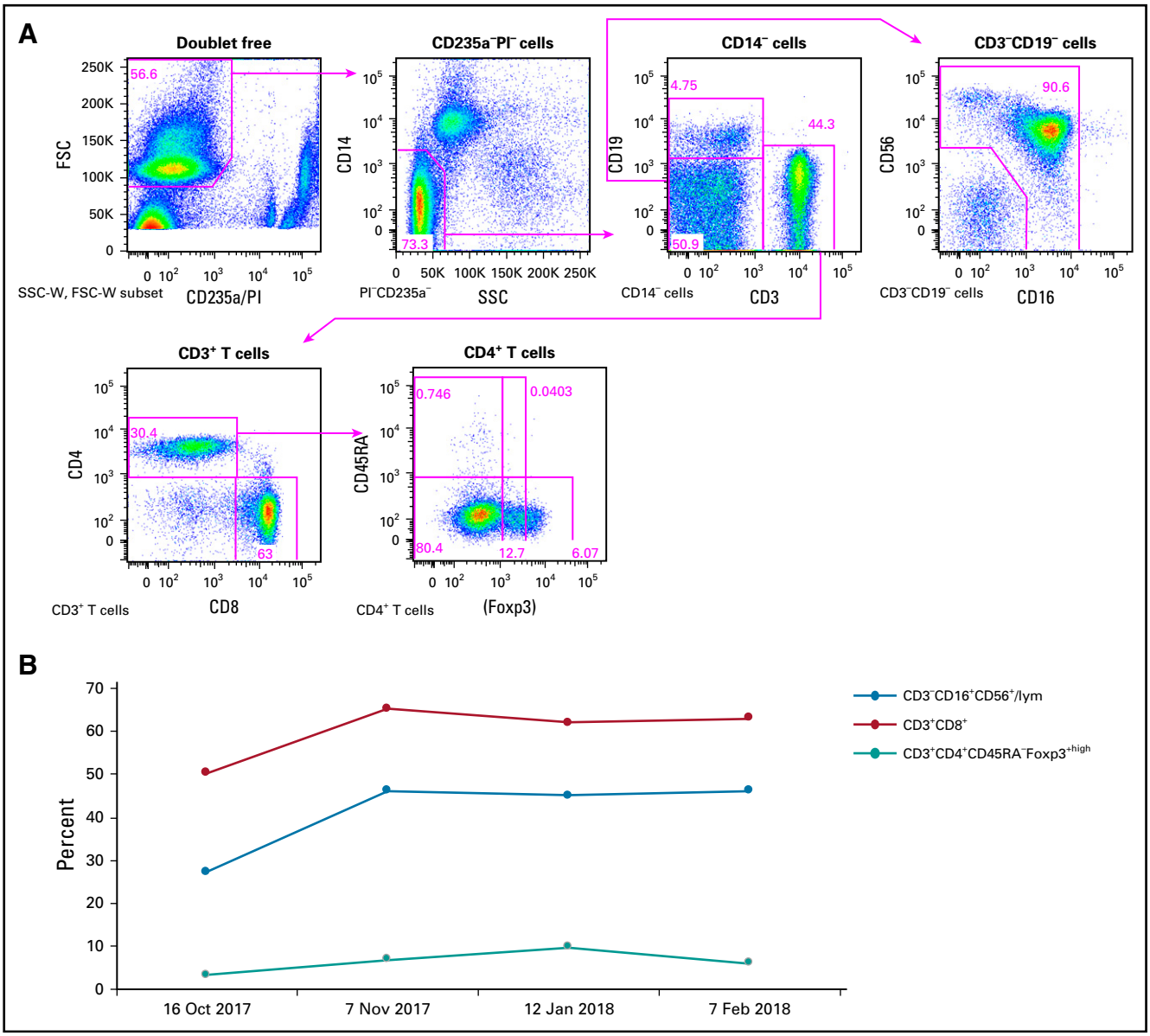

FIG A11. Immunophenotypes of peripheral blood mononuclear cells (PBMNCs) from the patient during lenalidomide treatment. PBMNCs were stained for CD3, CD4, CD8, CD14, CD16, CD19, CD45RA, CD235a/PI, and Foxp3. (A) Lymphocytes (lym) were identified based on light scatter characteristics (low forward and low side scatter) and negative for CD14 and CD235/PI. Natural killer (NK) cells were defined as $CD3^{-}CD16^{+}CD56^{+}$ after gating for $CD19^{-}$ lymphocytes. Effector regulatory T (Treg) cells were defined as $CD4^{+}CD45RA^{-}Foxp3^{+high}$. (B) The frequencies of NK cells and ratio of $CD3^{+}CD8^{+}$ T cells increased after lenalidomide treatment, which was not accompanied by an increase in effector Treg cells. FSC-W, forward scatter pulse width; SSC-W, side scatter pulse width.

TABLE A1. Coding Variants Identified From Whole-Exome Sequencing

Tier Grading (driver)	Chrom	Position	Ref	ALT	Depth (tumor)	Depth (normal)	VAF	$-\text{Log}_{10}$ P^a	Gene	Amino Acid Change	COSMIC70 ID	SIFT	PolyPhen-2	MutationTaster
1	17	7578290	C	T	90	148	0.567	25.1	*TP53*	splicing	COSM04139869	—	—	D
2 (VUS)	17	40312126	TCTGGCAC	T	148	134	0.074	3.0	*KCNH4*	p.P993fs	—	—	—	—
2 (VUS)	17	53007453	G	T	89	63	0.079	1.4	*TOM1L1*	p.R247L	—	D	D	D
2 (VUS)	4	187539038	G	T	164	133	0.104	4.4	*FAT1*	p.T2901K	—	T	P	D
2 (VUS)	18	7080421	C	T	123	98	0.122	3.8	*LAMA1*	p.A33T	—	T	D	D
2 (VUS)	3	126194576	C	G	43	52	0.140	2.2	*ZXDC*	p.G45R	—	D	B	N
2 (VUS)	17	72869018	G	A	43	53	0.140	2.2	*FDXR*	p.R18W	—	D	D	N
2 (VUS)	18	3215065	C	T	57	52	0.140	2.2	*MYOM1*	p.A53T	—	T	D	D
2 (VUS)	1	19951997	C	G	49	84	0.143	3.2	*MINOS1*	p.Q112E	—	—	—	—
2 (VUS)	2	96801104	C	A	97	79	0.144	3.5	*ASTL*	p.D77Y	—	D	D	N
2 (VUS)	13	28611393	G	T	125	113	0.144	5.2	*FLT3*	p.P413Q	—	T	D	D
2 (VUS)	2	166854673	G	A	102	117	0.147	4.1	*SCN1A*	p.P1451S	—	D	D	D
2 (VUS)	13	95363807	CGCGGCGGC GGCGGCGGC GGCA	C	60	67	0.150	3.1	*SOX21*	p.159_166del	—	—	—	—
2 (VUS)	4	121957868	G	A	99	81	0.152	3.0	*NDNF*	p.R420X	—	T	—	D
2 (VUS)	3	164732921	C	A	149	163	0.154	7.8	*SI*	p.C1330F	—	T	P	N
2 (VUS)	17	79661973	G	A	173	161	0.162	8.5	*HGS*	p.R332Q	COSM3388305	T	D	D
2 (VUS)	9	13125277	TT	T	115	101	0.165	5.5	*MPDZ*	p.K1582fs	—	—	—	—
2 (VUS)	17	39537460	G	T	157	123	0.166	6.7	*KRT34*	p.Q188K	—	D	B	N
2 (VUS)	3	36873472	A	T	121	134	0.174	7.2	*TRANK1*	p.C2490X	—	T	—	A
2 (VUS)	9	95267818	AAATAG	A	134	137	0.179	7.8	*ECM2*	p.S486fs	—	—	—	—
2 (VUS)	X	15591554	GG	G	53	43	0.189	2.7	*ACE2*	p.P492fs	—	—	—	—
2 (VUS)	1	19952061	C	T	63	74	0.190	4.3	*MINOS1*	p.S133F	—	—	—	—
2 (VUS)	16	89657421	C	T	184	161	0.196	8.3	*CPNE7*	p.H450Y	—	D	D	D
2 (VUS)	18	70526084	G	A	85	76	0.212	4.3	*NETO1*	p.S149L	—	T	D	D
2 (VUS)	3	53535680	A	T	61	55	0.213	3.8	*CACNA1D*	p.N139I	—	D	D	D
2 (VUS)	1	78430824	C	A	121	149	0.215	7.4	*FUBP1*	p.E189X	—	T	—	A
2 (VUS)	1	237802393	G	T	73	127	0.219	7.5	*RYR2*	p.R2336I	—	D	D	D
2 (VUS)	8	3265685	C	T	182	138	0.220	9.1	*CSMD1*	p.E603K	—	T	D	D
2 (VUS)	11	93553992	CACAGCAGCG	C	93	96	0.226	7.0	*VSTM5*	p.156_159del	—	—	—	—
2 (VUS)	1	11584044	C	T	48	61	0.229	4.2	*PTCHD2*	p.T803M	—	D	D	D
2 (VUS)	1	46650954	G	T	55	48	0.255	4.2	*TSPAN1*	p.V218L	—	T	D	D
2 (VUS)	12	8672843	AGATA	A	120	132	0.258	11.0	*CLEC4D*	p.D136fs	—	—	—	—

(Continued on following page)

TABLE A1. Coding Variants Identified From Whole-Exome Sequencing (Continued)

Tier Grading (driver)	Chrom	Position	Ref	ALT	Depth (tumor)	Depth (normal)	VAF	$-\text{Log}_{10}$ P^a	Gene	Amino Acid Change	COSMIC70 ID	SIFT	PolyPhen-2	MutationTaster
2 (VUS)	20	644532	C	G	25	34	0.280	2.9	*SCRT2*	p.G236A	—	D	D	D
2 (VUS)	19	15806829	G	A	151	136	0.285	12.0	*CYP4F12*	p.R400Q	—	D	D	N
2 (VUS)	17	39221748	G	T	122	128	0.287	12.2	*KRTAP2-4*	p.T117N	—	T	—	N
2 (VUS)	1	46650955	T	A	52	42	0.288	4.1	*TSPAN1*	p.V218E	—	D	D	D
2 (VUS)	17	20156852	G	T	51	74	0.294	5.4	*SPECC1*	p.S878I	COSM1609946	T	D	D
2 (VUS)	8	103287953	C	T	155	113	0.297	12.4	*UBR5*	p.G2205R	—	D	D	D
2 (VUS)	14	80271480	C	A	121	90	0.298	9.8	*NRXN3*	p.S944Y	—	—	D	D
2 (VUS)	20	43353525	A	G	41	32	0.317	3.5	*WISP2*	p.S142G	—	T	P	N
2 (VUS)	X	13863326	A	T	112	86	0.321	10.0	*F9*	p.K188X	—	T	—	A
2 (VUS)	7	2963954	G	T	109	88	0.330	10.5	*CARD11*	p.S618Y	—	D	D	D
2 (VUS)	3	135871427	A	G	97	107	0.340	12.1	*MSL2*	p.L99P	—	D	B	D
2 (VUS)	19	53518131	A	G	211	213	0.341	23.4	*ERVV-1*	p.N263S	—	—	—	—
2 (VUS)	2	186609095	C	G	70	101	0.343	10.5	*FSIP2*	p.T234S	—	D	—	N
2 (VUS)	21	47627432	C	A	42	72	0.357	6.2	*LSS*	p.E379D	—	D	D	D
2 (VUS)	5	42797023	G	A	53	63	0.377	7.8	*CCDC152*	p.E175K	—	T	P	D
2 (VUS)	7	73011983	G	T	46	48	0.391	6.5	*MLXIPL*	p.L378I	—	T	D	N
2 (VUS)	19	44096699	G	A	51	29	0.392	4.6	*IRGQ*	p.P451S	—	T	D	N
2 (VUS)	7	2963955	A	G	114	88	0.404	13.3	*CARD11*	p.S618P	—	D	D	D
2 (VUS)	15	48055295	A	T	71	116	0.408	12.8	*SEMA6D*	p.L247F	—	D	D	D
2 (VUS)	19	46915685	C	T	156	156	0.410	19.6	*CCDC8*	p.R128H	—	D	D	D
2 (VUS)	11	68369416	C	CC	98	67	0.429	8.0	*PPP6R3*	p.A760fs	—	—	—	—
2 (VUS)	12	56481867	C	A	77	78	0.455	12.8	*ERBB3*	p.Y265X	—	T	—	D
2 (VUS)	18	76755235	G	A	83	83	0.458	13.5	*SALL3*	p.A1082T	COSM3388512	T	P	N
2 (VUS)	7	39046468	G	A	91	80	0.462	14.0	*POU6F2*	splicing	—	—	—	N
2 (VUS)	12	32137570	GTGT	G	51	47	0.471	8.3	*KIAA1551*	p.1228_1228del	—	—	—	—
2 (VUS)	6	42993008	G	A	72	103	0.472	15.7	*RRP36*	p.E96K	—	D	D	D
2 (VUS)	3	37783231	G	A	92	123	0.478	18.1	*ITGA9*	p.E749K	—	T	P	D
2 (VUS)	7	138356846	T	C	113	62	0.478	12.9	*SVOPL*	p.E64G	—	T	P	D
2 (VUS)	3	111997701	G	A	68	51	0.485	9.9	*SLC9C1*	p.Q65X	—	T	—	A
2 (VUS)	12	21919331	C	T	113	135	0.487	22.9	*KCNJ8*	p.V201I	—	T	P	D
2 (VUS)	4	152198352	C	A	53	39	0.491	7.5	*PRSS48*	p.L10M	—	T	D	N
2 (VUS)	2	218713130	G	A	169	151	0.497	27.1	*TNS1*	p.R579W	—	D	D	D

(Continued on following page)

TABLE A1. Coding Variants Identified From Whole-Exome Sequencing (Continued)

Tier Grading (driver)	Chrom	Position	Ref	ALT	Depth (tumor)	Depth (normal)	VAF	$-\text{Log}_{10}$ P[a]	Gene	Amino Acid Change	COSMIC70 ID	SIFT	PolyPhen-2	MutationTaster
2 (VUS)	4	124323293	C	G	95	83	0.505	16.1	*SPRY1*	p.Q183E	—	—	B	D
2 (VUS)	4	159780304	C	T	106	111	0.509	19.1	*FNIP2*	p.S318F	—	—	P	D
2 (VUS)	11	78369497	C	T	128	103	0.516	19.7	*TENM4*	p.R2639Q	—	—	D	D
2 (VUS)	11	125359439	C	T	95	99	0.516	18.9	*FEZ1*	p.A79T	COSM1725252	T	P	D
2 (VUS)	11	59604724	G	A	154	129	0.519	26.7	*GIF*	p.P265L	—	T	P	D
2 (VUS)	11	55904379	C	A	152	149	0.546	29.6	*OR8J3*	p.K272N	—	D	D	N
2 (VUS)	17	18110149	G	A	42	72	0.548	12.2	*ALKBH5*	p.R291Q	—	T	D	D
2 (VUS)	6	13697092	C	A	51	62	0.569	12.7	*RANBP9*	p.R203L	—	D	D	D
2 (VUS)	22	19753291	T	G	30	56	0.600	9.0	*TBX1*	p.L284R	—	D	D	D
2 (VUS)	5	140202978	G	T	89	145	0.607	27.2	*PCDHA5*	p.G540C	—	D	D	D
2 (VUS)	10	105344436	CGCCGCGCCG GCC	C	59	129	0.627	21.9	*NEURL1*	p.265_269del	—	—	—	—
2 (VUS)	3	98251931	A	T	62	67	0.629	16.4	*GPR15*	p.R352W	—	D	D	D
2 (VUS)	9	20414179	G	A	191	208	0.707	58.5	*MLLT3*	p.S222F	—	D	D	D

Abbreviations: A (MutationTaster), disease causing automatic; B (Polyphen-2), benign; Chrom, chromosome; COSMIC70 ID, Catalog of Somatic Mutations in Cancer version 70 identifier; D (MutationTaster), disease causing; D (Polyphen-2), damaging; D (SIFT), deleterious; N (MutationTaster), polymorphism; P (MutationTaster), polymorphism automatic; P (Polyphen-2), possibly or probably damaging; SIFT, Sorting Intolerant From Tolerant; T (SIFT), tolerated; VAF, variant allele frequency; VUS, variant of unknown significance.

[a]Fisher's exact test.

TABLE A2. Clinical Characteristics of the Two Patients With ATL in the Study

UPN	Diagnosis	ATL-PI	Sex	Age (years)	Clinical Stage	Best Clinical Response to Lenalidomide	Lenalidomide Dose at Best Response (mg)
1	ATL, acute type	Intermediate	Male	67	IV	PR	20
2	ATL, acute type	Intermediate	Female	58	IV	PD	20

Abbreviations: ATL, adult T-cell leukemia/lymphoma; PI, prognostic index; PR, partial response; PD, progressive disease; UPN, unique patient number.

TABLE A3. Result of KEGG Pathway Enrichment Analysis of CTCL and ATL by DAVID

Sample	Category	Term	No.	%	*P*	Benjamini
ATL	KEGG_PATHWAY	Acute myeloid leukemia	15	1.3	2.20E-04	1.90E-03
CTCL	KEGG_PATHWAY	African trypanosomiasis	7	0.6	6.50E-02	2.30E-01
ATL	KEGG_PATHWAY	African trypanosomiasis	8	0.7	2.10E-02	7.70E-02
CTCL	KEGG_PATHWAY	Alcoholism	56	4.5	7.60E-18	9.80E-16
ATL	KEGG_PATHWAY	Allograft rejection	15	1.3	1.10E-06	1.90E-05
CTCL	KEGG_PATHWAY	Allograft rejection	18	1.4	2.70E-09	7.00E-08
ATL	KEGG_PATHWAY	Amino sugar and nucleotide sugar metabolism	10	0.8	2.00E-02	7.70E-02
CTCL	KEGG_PATHWAY	Amoebiasis	16	1.3	4.40E-02	1.70E-01
ATL	KEGG_PATHWAY	Amoebiasis	20	1.7	1.70E-03	1.00E-02
ATL	KEGG_PATHWAY	Amyotrophic lateral sclerosis	11	0.9	9.50E-03	4.20E-02
ATL	KEGG_PATHWAY	Antigen processing and presentation	20	1.7	1.70E-05	2.00E-04
CTCL	KEGG_PATHWAY	Antigen processing and presentation	26	2.1	2.60E-09	7.60E-08
ATL	KEGG_PATHWAY	**Apoptosis**	10	0.8	8.50E-02	2.40E-01
CTCL	KEGG_PATHWAY	**Apoptosis**	14	1.1	2.40E-03	1.50E-02
ATL	KEGG_PATHWAY	Asthma	12	1.0	2.20E-05	2.50E-04
CTCL	KEGG_PATHWAY	Asthma	14	1.1	4.90E-07	5.50E-06
ATL	KEGG_PATHWAY	Autoimmune thyroid disease	15	1.3	9.20E-05	9.30E-04
CTCL	KEGG_PATHWAY	Autoimmune thyroid disease	20	1.6	3.20E-08	5.40E-07
ATL	KEGG_PATHWAY	B-cell receptor signaling pathway	15	1.3	2.00E-03	1.20E-02
CTCL	KEGG_PATHWAY	B-cell receptor signaling pathway	18	1.4	6.90E-05	5.00E-04
CTCL	KEGG_PATHWAY	Bacterial invasion of epithelial cells	15	1.2	7.40E-03	3.90E-02
ATL	KEGG_PATHWAY	Bladder cancer	11	0.9	2.10E-03	1.20E-02
ATL	KEGG_PATHWAY	Cell adhesion molecules	23	1.9	5.10E-03	2.40E-02
CTCL	KEGG_PATHWAY	Cell adhesion molecules	36	2.9	1.10E-08	2.60E-07
CTCL	KEGG_PATHWAY	Cell cycle	31	2.5	2.00E-07	2.40E-06
ATL	KEGG_PATHWAY	Central carbon metabolism in cancer	11	0.9	4.70E-02	1.50E-01
CTCL	KEGG_PATHWAY	Chagas disease (American trypanosomiasis)	17	1.4	1.90E-02	8.50E-02
ATL	KEGG_PATHWAY	Chagas disease (American trypanosomiasis)	22	1.8	1.80E-04	1.60E-03
ATL	KEGG_PATHWAY	Chemokine signaling pathway	37	3.1	2.90E-06	4.00E-05
CTCL	KEGG_PATHWAY	Chemokine signaling pathway	39	3.1	5.30E-07	5.80E-06
ATL	KEGG_PATHWAY	Chronic myeloid leukemia	16	1.3	1.10E-03	6.70E-03
ATL	KEGG_PATHWAY	Collecting duct acid secretion	8	0.7	6.80E-03	3.10E-02
CTCL	KEGG_PATHWAY	Colorectal cancer	10	0.8	9.10E-02	2.90E-01
ATL	KEGG_PATHWAY	Colorectal cancer	12	1.0	1.60E-02	6.40E-02
ATL	KEGG_PATHWAY	Complement and coagulation cascades	13	1.1	1.40E-02	5.90E-02
ATL	KEGG_PATHWAY	**Cytokine-cytokine receptor interaction**	31	2.6	2.90E-02	1.00E-01
CTCL	KEGG_PATHWAY	**Cytokine-cytokine receptor interaction**	38	3.0	6.10E-04	4.00E-03
CTCL	KEGG_PATHWAY	Cytosolic DNA-sensing pathway	11	0.9	5.10E-02	1.90E-01
CTCL	KEGG_PATHWAY	DNA replication	16	1.3	1.20E-07	1.60E-06
ATL	KEGG_PATHWAY	Dorsoventral axis formation	6	0.5	7.90E-02	2.30E-01
ATL	KEGG_PATHWAY	Endocytosis	30	2.5	4.30E-02	1.40E-01
CTCL	KEGG_PATHWAY	Endocytosis	32	2.6	1.90E-02	8.70E-02
ATL	KEGG_PATHWAY	Endometrial cancer	11	0.9	1.20E-02	5.20E-02
ATL	KEGG_PATHWAY	Epithelial cell signaling in *Helicobacter pylori* infection	14	1.2	4.30E-03	2.20E-02

(Continued on following page)

TABLE A3. Result of KEGG Pathway Enrichment Analysis of CTCL and ATL by DAVID (Continued)

Sample	Category	Term	No.	%	*P*	Benjamini
ATL	KEGG_PATHWAY	Epstein-Barr virus infection	25	2.1	1.00E-04	9.80E-04
CTCL	KEGG_PATHWAY	Epstein-Barr virus infection	35	2.8	5.60E-10	2.10E-08
ATL	KEGG_PATHWAY	ErbB signaling pathway	14	1.2	3.60E-02	1.20E-01
ATL	KEGG_PATHWAY	Estrogen signaling pathway	14	1.2	8.40E-02	2.40E-01
CTCL	KEGG_PATHWAY	Fanconi anemia pathway	9	0.7	9.00E-02	2.90E-01
CTCL	KEGG_PATHWAY	Fcε RI signaling pathway	14	1.1	5.60E-03	3.10E-02
ATL	KEGG_PATHWAY	Fcε RI signaling pathway	14	1.2	5.00E-03	2.40E-02
CTCL	KEGG_PATHWAY	Fcγ R-mediated phagocytosis	18	1.4	8.50E-04	5.50E-03
ATL	KEGG_PATHWAY	Fcγ R-mediated phagocytosis	23	1.9	1.60E-06	2.50E-05
CTCL	KEGG_PATHWAY	Focal adhesion	26	2.1	6.00E-02	2.20E-01
ATL	KEGG_PATHWAY	Focal adhesion	26	2.2	5.20E-02	1.60E-01
ATL	KEGG_PATHWAY	FoxO signaling pathway	20	1.7	2.20E-02	7.90E-02
ATL	KEGG_PATHWAY	Galactose metabolism	9	0.8	3.20E-03	1.70E-02
ATL	KEGG_PATHWAY	Glioma	12	1.0	2.30E-02	8.20E-02
ATL	KEGG_PATHWAY	Glutathione metabolism	12	1.0	3.60E-03	1.80E-02
ATL	KEGG_PATHWAY	GnRH signaling pathway	13	1.1	9.30E-02	2.60E-01
ATL	KEGG_PATHWAY	Graft-*v*-host disease	15	1.3	2.00E-07	5.30E-06
CTCL	KEGG_PATHWAY	Graft-*v*-host disease	16	1.3	2.80E-08	5.70E-07
ATL	KEGG_PATHWAY	**Hematopoietic cell lineage**	20	1.7	1.30E-04	1.10E-03
CTCL	KEGG_PATHWAY	**Hematopoietic cell lineage**	22	1.8	1.40E-05	1.10E-04
CTCL	KEGG_PATHWAY	Hepatitis B	24	1.9	3.70E-03	2.10E-02
ATL	KEGG_PATHWAY	Hepatitis B	29	2.4	3.80E-05	4.00E-04
ATL	KEGG_PATHWAY	Hepatitis C	21	1.8	1.00E-02	4.40E-02
ATL	KEGG_PATHWAY	Herpes simplex infection	35	2.9	1.40E-05	1.60E-04
CTCL	KEGG_PATHWAY	Herpes simplex infection	42	3.4	1.20E-08	2.60E-07
ATL	KEGG_PATHWAY	HIF-1 signaling pathway	20	1.7	4.80E-04	3.50E-03
ATL	KEGG_PATHWAY	**HTLV-1 infection**	37	3.1	2.00E-03	1.20E-02
CTCL	KEGG_PATHWAY	**HTLV-1 infection**	62	5.0	9.90E-14	6.40E-12
CTCL	KEGG_PATHWAY	Inflammatory bowel disease	20	1.6	1.30E-06	1.30E-05
ATL	KEGG_PATHWAY	Inflammatory bowel disease	20	1.7	1.00E-06	2.00E-05
CTCL	KEGG_PATHWAY	Inflammatory mediator regulation of TRP channels	14	1.1	8.70E-02	2.90E-01
CTCL	KEGG_PATHWAY	Influenza A	35	2.8	6.00E-06	4.90E-05
ATL	KEGG_PATHWAY	Influenza A	44	3.7	1.20E-10	4.10E-09
ATL	KEGG_PATHWAY	Insulin signaling pathway	21	1.8	1.50E-02	6.10E-02
ATL	KEGG_PATHWAY	Intestinal immune network for IgA production	16	1.3	5.30E-06	7.10E-05
CTCL	KEGG_PATHWAY	Intestinal immune network for IgA production	19	1.5	3.10E-08	5.70E-07
CTCL	KEGG_PATHWAY	JAK-STAT signaling pathway	21	1.7	2.80E-02	1.20E-01
CTCL	KEGG_PATHWAY	Legionellosis	9	0.7	9.80E-02	3.10E-01
ATL	KEGG_PATHWAY	Legionellosis	14	1.2	5.40E-04	3.90E-03
CTCL	KEGG_PATHWAY	Leishmaniasis	23	1.8	8.20E-08	1.20E-06
ATL	KEGG_PATHWAY	Leishmaniasis	35	2.9	2.80E-18	2.40E-16
ATL	KEGG_PATHWAY	Leukocyte transendothelial migration	23	1.9	2.90E-04	2.40E-03
CTCL	KEGG_PATHWAY	Leukocyte transendothelial migration	27	2.2	5.00E-06	4.30E-05
ATL	KEGG_PATHWAY	Long-term potentiation	11	0.9	5.60E-02	1.70E-01

(Continued on following page)

TABLE A3. Result of KEGG Pathway Enrichment Analysis of CTCL and ATL by DAVID (Continued)

Sample	Category	Term	No.	%	*P*	Benjamini
CTCL	KEGG_PATHWAY	Lysosome	18	1.4	3.50E-02	1.40E-01
ATL	KEGG_PATHWAY	Lysosome	46	3.8	1.90E-18	2.60E-16
CTCL	KEGG_PATHWAY	Malaria	10	0.8	2.50E-02	1.10E-01
ATL	KEGG_PATHWAY	Malaria	17	1.4	1.80E-06	2.70E-05
ATL	KEGG_PATHWAY	MAPK signaling pathway	35	2.9	6.30E-03	2.90E-02
ATL	KEGG_PATHWAY	Measles	25	2.1	3.90E-04	3.10E-03
CTCL	KEGG_PATHWAY	Measles	31	2.5	9.90E-07	1.00E-05
CTCL	KEGG_PATHWAY	Mismatch repair	9	0.7	5.10E-04	3.50E-03
ATL	KEGG_PATHWAY	**NK-cell–mediated cytotoxicity**	29	2.4	1.20E-06	1.90E-05
CTCL	KEGG_PATHWAY	**NK-cell–mediated cytotoxicity**	30	2.4	4.70E-07	5.50E-06
ATL	KEGG_PATHWAY	Neurotrophin signaling pathway	20	1.7	7.00E-03	3.20E-02
ATL	KEGG_PATHWAY	**NF-κB signaling pathway**	19	1.6	3.80E-04	3.10E-03
CTCL	KEGG_PATHWAY	**NF-κB signaling pathway**	32	2.6	2.90E-12	1.50E-10
ATL	KEGG_PATHWAY	NOD-like receptor signaling pathway	14	1.2	7.80E-04	5.30E-03
ATL	KEGG_PATHWAY	Non–small-cell lung cancer	10	0.8	5.00E-02	1.60E-01
CTCL	KEGG_PATHWAY	Oocyte meiosis	19	1.5	7.70E-03	4.00E-02
CTCL	KEGG_PATHWAY	Osteoclast differentiation	33	2.6	6.00E-08	9.10E-07
ATL	KEGG_PATHWAY	Osteoclast differentiation	45	3.8	5.00E-16	2.50E-14
ATL	KEGG_PATHWAY	Other glycan degradation	6	0.5	1.60E-02	6.30E-02
CTCL	KEGG_PATHWAY	**p53 signaling pathway**	13	1.0	1.30E-02	6.20E-02
ATL	KEGG_PATHWAY	Pancreatic cancer	14	1.2	3.30E-03	1.70E-02
CTCL	KEGG_PATHWAY	Pathogenic *Escherichia coli* infection	13	1.0	1.20E-03	7.80E-03
ATL	KEGG_PATHWAY	Pathways in cancer	43	3.6	8.40E-02	2.50E-01
CTCL	KEGG_PATHWAY	Pathways in cancer	49	3.9	1.10E-02	5.60E-02
ATL	KEGG_PATHWAY	Pentose phosphate pathway	7	0.6	3.50E-02	1.20E-01
CTCL	KEGG_PATHWAY	Pertussis	14	1.1	1.30E-02	6.10E-02
ATL	KEGG_PATHWAY	Pertussis	22	1.8	8.30E-07	1.70E-05
CTCL	KEGG_PATHWAY	Phagosome	33	2.6	1.60E-06	1.50E-05
ATL	KEGG_PATHWAY	Phagosome	49	4.1	1.50E-16	7.30E-15
ATL	KEGG_PATHWAY	Platelet activation	26	2.2	1.10E-04	1.00E-03
CTCL	KEGG_PATHWAY	Platelet activation	29	2.3	5.90E-06	4.90E-05
CTCL	KEGG_PATHWAY	Primary immunodeficiency	16	1.3	4.70E-08	7.60E-07
ATL	KEGG_PATHWAY	Prion diseases	11	0.9	4.30E-04	3.20E-03
CTCL	KEGG_PATHWAY	Progesterone-mediated oocyte maturation	16	1.3	8.30E-03	4.20E-02
ATL	KEGG_PATHWAY	Prolactin signaling pathway	13	1.1	1.80E-02	6.90E-02
CTCL	KEGG_PATHWAY	Protein processing in endoplasmic reticulum	27	2.2	3.30E-03	1.90E-02
CTCL	KEGG_PATHWAY	Proteoglycans in cancer	25	2.0	7.20E-02	2.50E-01
ATL	KEGG_PATHWAY	Proteoglycans in cancer	32	2.7	9.60E-04	6.30E-03
ATL	KEGG_PATHWAY	Rap1 signaling pathway	27	2.3	3.90E-02	1.30E-01
CTCL	KEGG_PATHWAY	Rap1 signaling pathway	29	2.3	1.70E-02	7.70E-02
CTCL	KEGG_PATHWAY	Regulation of actin cytoskeleton	26	2.1	7.20E-02	2.50E-01
ATL	KEGG_PATHWAY	Regulation of actin cytoskeleton	32	2.7	2.10E-03	1.20E-02
CTCL	KEGG_PATHWAY	Rheumatoid arthritis	23	1.8	4.70E-06	4.20E-05
ATL	KEGG_PATHWAY	Rheumatoid arthritis	31	2.6	1.60E-11	6.10E-10

(Continued on following page)

TABLE A3. Result of KEGG Pathway Enrichment Analysis of CTCL and ATL by DAVID (Continued)

Sample	Category	Term	No.	%	*P*	Benjamini
CTCL	KEGG_PATHWAY	**RIG-I–like receptor signaling pathway**	11	0.9	8.40E-02	2.80E-01
CTCL	KEGG_PATHWAY	*Salmonella* infection	14	1.1	2.80E-02	1.20E-01
ATL	KEGG_PATHWAY	*Salmonella* infection	18	1.5	6.20E-04	4.30E-03
CTCL	KEGG_PATHWAY	Shigellosis	12	1.0	2.20E-02	9.80E-02
ATL	KEGG_PATHWAY	Sphingolipid signaling pathway	18	1.5	2.90E-02	1.00E-01
CTCL	KEGG_PATHWAY	*Staphylococcus aureus* infection	17	1.4	9.30E-06	7.30E-05
ATL	KEGG_PATHWAY	*S aureus* infection	29	2.4	2.00E-16	1.20E-14
ATL	KEGG_PATHWAY	Starch and sucrose metabolism	8	0.7	2.10E-02	7.70E-02
ATL	KEGG_PATHWAY	Systemic lupus erythematosus	23	1.9	2.40E-03	1.30E-02
CTCL	KEGG_PATHWAY	Systemic lupus erythematosus	67	5.4	3.80E-35	9.80E-33
CTCL	KEGG_PATHWAY	**T-cell receptor signaling pathway**	31	2.5	8.40E-10	2.70E-08
ATL	KEGG_PATHWAY	Thyroid cancer	8	0.7	1.00E-02	4.40E-02
CTCL	KEGG_PATHWAY	**TNF signaling pathway**	20	1.6	2.20E-03	1.40E-02
ATL	KEGG_PATHWAY	**TNF signaling pathway**	20	1.7	1.90E-03	1.10E-02
CTCL	KEGG_PATHWAY	**Toll-like receptor signaling pathway**	19	1.5	4.70E-03	2.60E-02
ATL	KEGG_PATHWAY	**Toll-like receptor signaling pathway**	27	2.3	7.20E-07	1.70E-05
CTCL	KEGG_PATHWAY	Toxoplasmosis	29	2.3	1.60E-07	2.10E-06
ATL	KEGG_PATHWAY	Toxoplasmosis	30	2.5	3.00E-08	8.80E-07
ATL	KEGG_PATHWAY	Transcriptional misregulation in cancer	28	2.3	1.10E-03	6.80E-03
CTCL	KEGG_PATHWAY	Transcriptional misregulation in cancer	30	2.4	2.60E-04	1.80E-03
CTCL	KEGG_PATHWAY	Tuberculosis	33	2.6	5.80E-05	4.30E-04
ATL	KEGG_PATHWAY	Tuberculosis	59	4.9	2.50E-20	6.50E-18
ATL	KEGG_PATHWAY	Type 1 diabetes mellitus	15	1.3	6.20E-06	7.80E-05
CTCL	KEGG_PATHWAY	Type 1 diabetes mellitus	16	1.3	1.30E-06	1.30E-05
ATL	KEGG_PATHWAY	*Vibrio cholerae* infection	11	0.9	1.20E-02	5.20E-02
CTCL	KEGG_PATHWAY	Viral carcinogenesis	58	4.6	6.30E-16	5.80E-14
ATL	KEGG_PATHWAY	Viral myocarditis	19	1.6	7.30E-07	1.60E-05
CTCL	KEGG_PATHWAY	Viral myocarditis	25	2.0	1.40E-11	5.90E-10

NOTE. Related to Figure A3. Bold indicates lenalidomide-related pathways, depicted either in public database from KEGG DRUG 7 or from Therapeutic Target Database8.

Abbreviations: ATL, adult T-cell leukemia/lymphoma; CTCL, cutaneous T-cell lymphoma; GnRH, gonadotropin-releasing hormone; Ig, immunoglobulin; JAK-STAT, Janus kinase–signal transducers and activators of transcription; KEGG, Kyoto Encyclopedia of Genes and Genomes; MAPK, mitogen-activated protein kinase; NK, natural killer; NF-κB, nuclear factor-κB; TNF, tumor necrosis factor.

TABLE A4. Immunohistochemical Analysis of Tumor Specimen

Specimen	CD8/HPF	CD25/HPF	Foxp3/HPF
Prelenalidomide treatment	31	2	2
After the first treatment cycle	122	1	5
After the third treatment cycle	27	1	0

Abbreviation: HPF, high-power field.

